

# Forecasting range shifts of a dioecious plant species under climate change

Jacob K. Moutouama 0000-0003-1599-1671<sup>\*1</sup>, Aldo Compagnoni 0000-0001-8302-7492<sup>2</sup>, and Tom E.X. Miller 0000-0003-3208-6067<sup>1</sup>

<sup>1</sup>Program in Ecology and Evolutionary Biology, Department of BioSciences, Rice University, Houston, Texas, USA

<sup>2</sup>Institute

of Biology, Martin Luther University Halle-Wittenberg, Halle, Germany; and German Centre for Integrative Biodiversity Research (iDiv), Leipzig, Germany

**Running header:** Forecasting range shifts

**Keywords:** demography, forecasting, global warming, matrix projection model, population dynamics, sex ratio, range limits

**Submitted to:** *Ecology letters* (Letter)

**Data accessibility statement:** All data used in this paper are publicly available and cited appropriately (Miller and Compagnoni, 2022a). Should the paper be accepted, all computer scripts supporting the results will be archived in a Zenodo package, with the DOI included at the end of the article. During peer review, our code (Stan and R) is available at <https://github.com/jmoutouama/POAR-Forecasting>.

**Conflict of interest statement:** None.

**Authorship statement:** J.K.M., A.C. and T.E.X.M. designed the study. A.C. and T.E.X.M. collected the data. All authors conducted the statistical analyses and modeling. J.K.M. drafted the manuscript, and T.E.X.M contributed to revisions.

**Abstract:**

**Main Text:**

**Figures:** 6

**Tables:** 0

**References:** 106

---

\*Corresponding author: jmoutouama@gmail.com

## <sup>1</sup> Abstract

<sup>2</sup> Global climate change has triggered an urgent need for predicting the reorganization of Earth's  
<sup>3</sup> biodiversity. Currently, the vast majority of models used to forecast population viability and  
<sup>4</sup> range shifts in response to climate change ignore the complication of sex structure, and thus  
<sup>5</sup> the potential for females and males to differ in their sensitivity to climate drivers. We developed  
<sup>6</sup> demographic models of range limitation, parameterized from geographically distributed com-  
<sup>7</sup> mon garden experiments, with females and males of a dioecious grass species (*Poa arachnifera*)  
<sup>8</sup> throughout and beyond its range in the south-central U.S. Female-dominant and two-sex  
<sup>9</sup> model versions both predict that future climate change will alter population viability and  
<sup>10</sup> will induce a poleward niche shift beyond current northern limits. However, the magnitude of  
<sup>11</sup> niche shift was underestimated by the female-dominant model, because females have broader  
<sup>12</sup> temperature tolerance than males and become mate-limited under female-biased sex ratios.  
<sup>13</sup> Our result illustrate how explicit accounting for both sexes could enhance population viability  
<sup>14</sup> forecasts and conservation planning for dioecious species in response to climate change.

15 **Introduction**

16 Rising temperatures and extreme drought events associated with global climate change are  
17 leading to increased concern about how species will become redistributed across the globe  
18 under future climate conditions (Bertrand et al., 2011; Gamelon et al., 2017; Smith et al., 2024).  
19 Species' range limits, when not driven by dispersal limitation, should generally reflect the limits  
20 of the ecological niche (Lee-Yaw et al., 2016). Niches and geographic ranges are often limited  
21 by climatic factors including temperature and precipitation (Sexton et al., 2009). Therefore,  
22 any substantial changes in the magnitude of these climatic factors could impact population  
23 viability, with implications for range expansions or contractions based on which regions of  
24 a species' range become more or less suitable (Davis and Shaw, 2001; Pease et al., 1989).

25 Forecasting range shifts for dioecious species (most animals and ca. 7% of plant species)  
26 is complicated by the potential for sexual niche differentiation, i.e. distinct responses of  
27 females and males to shared climate drivers (Hultine et al., 2016; Morrison et al., 2016; Pottier  
28 et al., 2021; Tognetti, 2012). The lower cost of reproduction for one sex (male or female)  
29 may allow that sex to invest its energy in other functions that produce higher growth rates,  
30 greater clonality, or even higher survival rates compared to the other sex, leading to sexual  
31 niche differentiation (Bruijning et al., 2017). Accounting for sexual niche differentiation  
32 is a long-standing challenge in accurately predicting which sex will successfully track  
33 environmental change and how this will impact population viability and range shifts (Gissi  
34 et al., 2023; Jones et al., 1999). Populations in which males are rare under current climatic  
35 conditions could experience low reproductive success due to sperm or pollen limitation that  
36 may lead to population decline in response to climate change that disproportionately favors  
37 females (Eberhart-Phillips et al., 2017). In contrast, climate change could expand male habitat  
38 suitability (e.g. upslope movement), which might increase seed set for mate-limited females  
39 and favor range expansion (Petry et al., 2016). Across dioecious plants, for example, studies  
40 suggest that future climate change toward hotter and drier conditions may favor male-biased  
41 sex ratios (Field et al., 2013; Hultine et al., 2016). Although the response of species to climate  
42 warming is an urgent and active area of research, few studies have disentangled the interaction  
43 between sex and climate drivers to understand their combined effects on population dynamics  
44 and range shifts, despite calls for such an approach (Gissi et al., 2023; Hultine et al., 2016).

45 The vast majority of theory and models in population biology, including those used  
46 to forecast biodiversity responses to climate change, ignore the complication of sex structure  
47 (but see Ellis et al., 2017; Gissi et al., 2024; Pottier et al., 2021). Traditional approaches instead  
48 focus exclusively on females, assuming that males are in sufficient supply as to never limit  
49 female fertility. In contrast, "two-sex" models are required to fully account for demographic

50 differences between females and males and sex-specific responses to shared climate drivers  
51 (Gerber and White, 2014; Miller et al., 2011). Sex differences in maturation, reproduction,  
52 and mortality schedules can generate skew in the operational sex ratio (OSR; sex ratio of  
53 individuals available for mating) even if the birth sex ratio is 1:1 (Eberhart-Phillips et al., 2017;  
54 Shelton, 2010). Climate and other environmental drivers can therefore influence the OSR  
55 via their influence on sex-specific demographic rates. In a two-sex framework, demographic  
56 rates both influence and respond to the OSR in a feedback loop that makes two-sex models  
57 inherently nonlinear and more data-hungry than corresponding female-dominant models.  
58 Given the additional complexity and data needs, forecasts of range dynamics for dioecious  
59 species under future climate change that explicitly account for females, males, and their  
60 inter-dependence are limited (Lynch et al., 2014; Petry et al., 2016).

61 Tracking the impact of climate change on population viability ( $\lambda$ ) and distributional  
62 limits of dioecious taxa depends on our ability to build mechanistic models that take into  
63 account the spatial and temporal context of sex specific response to climate change, while  
64 accounting for sources of uncertainty (Davis and Shaw, 2001; Evans et al., 2016). Structured  
65 population models built from demographic data collected from geographically distributed  
66 observations or common garden experiments provide several advantages for studying  
67 the impact of climate change on species' range shifts (Merow et al., 2017; Schultz et al.,  
68 2022; Schwinning et al., 2022). First, demographic models link individual-level life history  
69 events (mortality, development, and regeneration) to population demography, allowing the  
70 investigation of factors explaining vital rate responses to environmental drivers (Dahlgren  
71 et al., 2016; Ehrlén and Morris, 2015; Louthan et al., 2022). Second, demographic models  
72 have a natural interface with statistical estimation of individual-level vital rates that provide  
73 quantitative measures of uncertainty and isolate different sources of variation, features that  
74 can be propagated to population-level predictions (Elderd and Miller, 2016; Ellner et al.,  
75 2022). Finally, structured demographic models can be used to identify which aspects of  
76 climate are the most important drivers of population dynamics. For example, Life Table  
77 Response Experiments (LTRE) built from structured models have become widely used to  
78 understand the relative importance of covariates in explaining variation in population growth  
79 rate (Czachura and Miller, 2020; Ellner et al., 2016; Hernández et al., 2023).

80 In this study, we combined geographically-distributed common garden experiments,  
81 hierarchical Bayesian statistical modeling, two-sex population projection modeling, and climate  
82 back-casting and forecasting to understand demographic responses to climate change and their  
83 implications for past, present, and future range dynamics. Our work focused on the dioecious  
84 plant Texas bluegrass (*Poa arachnifera*), which is distributed along environmental gradients  
85 in the south-central U.S. corresponding to variation in temperature across latitude and

86 precipitation across longitude (Fig. 1A)<sup>1</sup>. This region has experienced rapid climate warming  
87 since 1900 and this is projected to continue through the end of the century (Fig. 1 B and C). Our  
88 previous study showed that, despite evidence for differentiation of climatic niche between sexes,  
89 the female niche mattered the most in driving longitudinal range limits of Texas bluegrass  
90 (Miller and Compagnoni, 2022b). However, that study used a single proxy variable (longitude)  
91 to represent environmental variation related to aridity and did not consider variation in  
92 temperature, which is the much stronger dimension of forecasted climate change in this region  
93 (Fig. S-2). Developing a rigorous forecast for the implications of future climate change requires  
94 that we transition from implicit to explicit treatment of multiple climate drivers, as we do  
95 here. Leveraging the power of Bayesian inference, we take a probabilistic view of past, present,  
96 and future range limits by quantifying the probability of population viability ( $Pr(\lambda \geq 1)$ ) in  
97 relation to climate drivers of demography, an approach that fully accounts for uncertainty  
98 arising from multiple sources of estimation and process error. Specifically, we asked:

- 99 1. What are the sex-specific vital rate responses to variation in temperature and precipitation  
100 across the species' range?
- 101 2. How do sex-specific vital rates combine to determine the influence of climate variation  
102 on population growth rate ( $\lambda$ )?
- 103 3. What is the impact of climate change on operational sex ratio throughout the range?
- 104 4. What are the likely historical and projected dynamics of the Texas bluegrass geographic  
105 niche and how does accounting for sex structure modify these predictions?

## 106 Materials and methods

### 107 Study species and climate context

108 Texas bluegrass (*Poa arachnifera*) is a dioecious perennial, summer-dormant cool-season (C3)  
109 grass that occurs in the south-central U.S. (Texas, Oklahoma, and southern Kansas) (Figure  
110 1) (Hitchcock, 1971). Texas bluegrass grows between October and May, flowers in spring,  
111 and goes dormant during the hot summer months of June to September (Kindiger, 2004).  
112 Following this life history, we divided the calendar year into growing (October 1 - May  
113 31) and dormant (June 1 - September 30) seasons in the analyses below. Biological sex is  
114 genetically based and the birth (seed) sex ratio is 1:1 (Renganayaki et al., 2005). Females and  
115 males are morphologically indistinguishable except for their inflorescences. Like all grasses,  
116 this species is wind pollinated (Hitchcock, 1971) and most male-female pollen transfer occurs

---

<sup>1</sup>Fig. A does not show what we are saying here. Maybe I should add the Figure with the raster

<sup>117</sup> within 10-15m (Compagnoni et al., 2017). Surveys of 22 natural populations throughout the  
<sup>118</sup> species' distribution indicated that operational sex ratio (the female fraction of inflorescences)  
<sup>119</sup> ranged from 0.007 to 0.986 with a mean of 0.404 (Miller and Compagnoni, 2022b).

<sup>120</sup> Latitudinal limits of the Texas bluegrass distribution span 7.74 °C to 16.94 °C of  
<sup>121</sup> temperature during the dormant season and 24.38 °C to 28.80 °C during the dormant season.  
<sup>122</sup> Longitudinal limits span 244.9 mm to 901.5 mm of precipitation during the growing season  
<sup>123</sup> and 156.3 mm to 373.3 mm. This region has experienced *ca.* 0.5 °C of climate warming since  
<sup>124</sup> 1900, with faster warming during the cool-season months ( $0.0055^{\circ}\text{C}/\text{yr}$ ) than the hot summers  
<sup>125</sup> ( $0.0046^{\circ}\text{C}/\text{yr}$ ) (Fig. S-1). Future warming is projected to accelerate to  $0.03 - 0.06^{\circ}\text{C}/\text{yr}$  by  
<sup>126</sup> the end of the century depending on the season and forecast model. On the other hand,  
<sup>127</sup> precipitation has increased over the past century for much of the region but is forecasted  
<sup>128</sup> to decline back to early-20th century levels (Fig. S-1). <sup>2</sup>

## <sup>129</sup> Common garden experiment

### <sup>130</sup> Experimental design

<sup>131</sup> We conducted a range-wide common garden experiment to quantify sex-specific demographic  
<sup>132</sup> responses to climate variation. Details of the experimental design are provided in Miller  
<sup>133</sup> and Compagnoni (2022b); we provide a brief overview here. The experiment was installed  
<sup>134</sup> at 14 sites throughout and, in some cases, beyond the natural range of Texas bluegrass that  
<sup>135</sup> sampled a broad range of latitude and longitude (Figure 1A). At each site, we established  
<sup>136</sup> 14 blocks. For each block we planted three female and three male individuals that were  
<sup>137</sup> clonally propagated from females and males from eight natural source populations (Figure  
<sup>138</sup> 1A); because sex is genetically-based, clones never deviated from their expected sex. The  
<sup>139</sup> experiment was established in November 2013 with a total of 588 female and 588 male plants,  
<sup>140</sup> and was censused in May of 2014, 2015, and 2016. At each census, we collected data on  
<sup>141</sup> survival, size (number of tillers), and number of panicles (reproductive inflorescences). For  
<sup>142</sup> the analyses that follow, we focus on the 2014-15 and 2015-16 transition years, since the start  
<sup>143</sup> of the experiment did not include the full 2013-14 transition year.

---

<sup>2</sup>*I like this but I don't know if this not a repetition of what we've said in the introduction about climate change in the study area.*

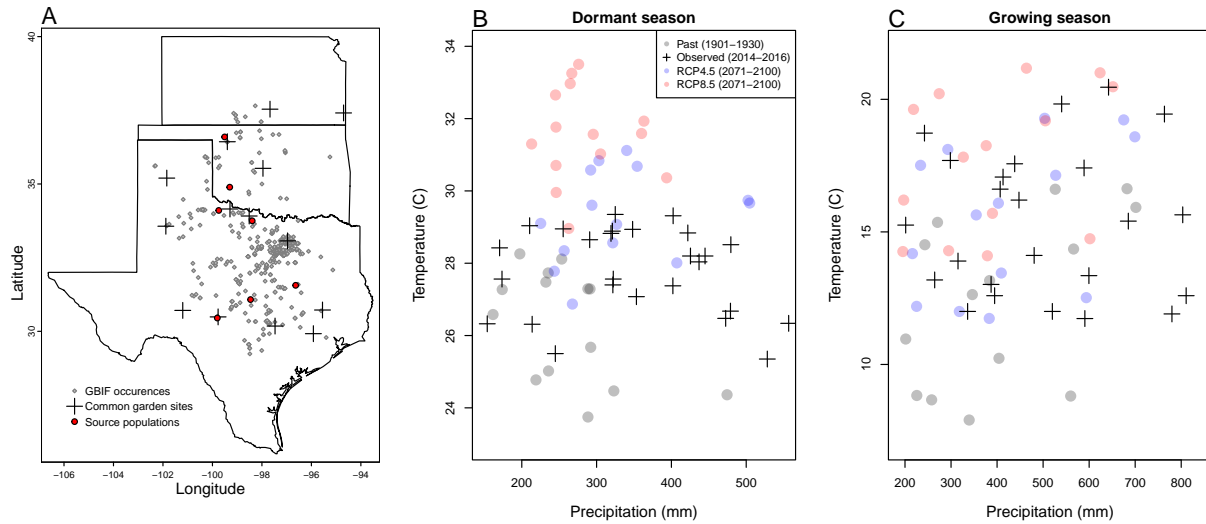


**Figure 1: Experimental gardens and climate of the study region.** **A:** Map of 14 experimental garden sites (crosses) in Texas, Oklahoma, and Kansas relative to GBIF occurrences of *Poa arachnifera* (gray points). Red points indicate source populations for plants used in the common garden experiment. **B,C:** Past, future, and observed climate space for growing and dormant seasons. Crosses show observed conditions for the sites and years of the common garden experiment. Gray points show historical (1901-1930) climate normals, and blue and red points show end-of-century (2071-2100) climate normals for RCP4.5 and RCP8.5 projections, respectively, from MIROC5. See also (Figure ?? for more information about historical and projected climate change in the study region.

#### 144 Climatic data collection

145 We gathered downscaled monthly temperature and precipitation for each site from Chelsa  
 146 (Karger et al., 2017) to describe observed climate conditions during our study period. These  
 147 climate data were used as covariates in vital rate regressions. We aligned the climatic years  
 148 to match demographic transition years (June 1 – May 31) and growing and dormant seasons  
 149 within each year. To back-cast and forecast demographic responses to changes in climate  
 150 throughout the study region, we also gathered projection data for three 30-year periods: “past”  
 151 (1901-1930), “current” (1990-2019) and “future” (2070-2100). Data for future climatic periods  
 152 were downloaded from four general circulation models (GCMs) selected from the Coupled  
 153 Model Intercomparison Project Phase 5 (CMIP5): Model for Interdisciplinary Research on  
 154 Climate (MIROC5), Australian Community Climate and Earth System Simulator (ACCESS1-3),  
 155 Community Earth System Model (CESM1-BGC), Centro Euro-Mediterraneo sui Cambiamenti  
 156 Climatici Climate Model (CMCC-CM). All the GCMs were also downloaded from Chelsa  
 157 (Sanderson et al., 2015). We evaluated future climate projections from two scenarios of  
 158 representative concentration pathways (RCPs): RCP4.5, an intermediate-to-pessimistic scenario  
 159 assuming a radiative forcing amounting to  $4.5 \text{ W m}^{-2}$  by 2100, and RCP8.5, a pessimistic

<sup>160</sup> emission scenario which projects a radiative forcing of  $8.5 \text{ Wm}^{-2}$  by 2100 (Schwalm et al.,  
<sup>161</sup> 2020; Thomson et al., 2011).

<sup>162</sup> Projection data for the three 30-year periods included warmer or colder conditions than ob-  
<sup>163</sup> served in our experiment, so extending our inferences to these conditions required some extrap-  
<sup>164</sup> olation. However, across all sites, both study years were 1-2°C warmer than their correspond-  
<sup>165</sup> ing “current” (1990-2019) temperature normals (Fig. S-2). Additionally, the 2014–15 growing  
<sup>166</sup> season was generally wetter and cooler across the study region than 2015–16 (Fig. S-2). Com-  
<sup>167</sup> bined, the geographic and inter-annual replication of the common garden experiment provided  
<sup>168</sup> good coverage of most past and future conditions throughout the study region (Fig. 1B,C).

### <sup>169</sup> **Sex-specific demographic responses to climatic variation across common garden sites**

<sup>170</sup> We used individual-level measurements of survival, growth (change in number of tillers), flow-  
<sup>171</sup> ering, and number of panicles (conditional on flowering) to develop Bayesian mixed effect mod-  
<sup>172</sup> els describing how each vital rate varies as a function of sex, size, and four climate covariates  
<sup>173</sup> (precipitation and temperature of growing and dormant season)(Supplementary Method S.2.1).  
<sup>174</sup> These vital rate models included main effects of size (the natural log of tiller number), sex, and  
<sup>175</sup> seasonal climate covariates. Climate variables were fit with second-degree polynomial func-  
<sup>176</sup> tions to accommodate the possibility of hump-shaped relationships (reduced demographic per-  
<sup>177</sup> formance at both extremes). We also included two-way interactions between sex and each cli-  
<sup>178</sup> mate driver and between temperature and precipitation within each season, and a three-way in-  
<sup>179</sup> teraction between sex, temperature, and precipitation within each season. We modeled survival  
<sup>180</sup> and flowering data with a Bernoulli distribution and the growth (tiller number) with a zero-  
<sup>181</sup> truncated Poisson inverse Gaussian distribution. Fertility (panicle count conditional on flower-  
<sup>182</sup> ing) was modeled as zero-truncated negative binomial. We used generic, weakly informative  
<sup>183</sup> priors to fit coefficients for survival, growth, flowering models ( $\beta \sim N(0, 1.5)$ ) and random  
<sup>184</sup> effect variances ( $\sigma \sim \text{Gamma}(\gamma(0.1, 0.1))$ ). We fit fertility model with also weakly informative pri-  
<sup>185</sup> ors for coefficients ( $\beta \sim N(0, 0.15)$ ). Different priors were used for fertility because the panicle  
<sup>186</sup> model has a large number of parameters relative to the amount of available data (subset of our  
<sup>187</sup> data) and because these specifics priors help prevent the model from overfitting. Each vital rate  
<sup>188</sup> also includes normally distributed random effects for block-to-block variation ( $\phi \sim N(0, \sigma_{block})$ ),  
<sup>189</sup> site to site variation ( $\nu \sim N(0, \sigma_{site})$ ), and source-to-source variation that is related to the genetic  
<sup>190</sup> provenance of the transplants used to establish the common garden ( $\rho \sim N(0, \sigma_{source})$ ).

191 **Sex ratio responses to climatic variation across common garden sites**

192 We also used the experimental data to investigate how climatic variation across the range  
193 influenced sex ratio and operational sex ratio of the common garden populations. To do so,  
194 we developed two Bayesian linear models using data collected during three years. Each model  
195 had OSR or SR as response variable and a climate variable (temperature and precipitation  
196 of the growing season and dormant season) as predictor (Supplementary Method S.2.2). We  
197 modeled the OSR or SR data with a Bernoulli distribution and used non informative priors  
198 for each coefficient ( $\omega \sim N(0, 100)$ ).

199 **Model-fitting procedures**

200 All models were fit using Stan (Stan Development Team, 2023) in R 4.3.1 (R Core Team,  
201 2023). We centered and standardized all climatic predictors to mean zero, variance one, which  
202 facilitated model convergence. We ran three chains for 1000 samples for warmup and 4000  
203 for sampling, with a thinning rate of 3. We assessed the quality of the models using posterior  
204 predictive checks (Piironen and Vehtari, 2017) (Figure S-3).

205 **Two-sex and female-dominant matrix projection models**

206 We used the climate-dependent vital rate regressions estimated above, combined with  
207 additional data sources, to build female-dominant and two-sex versions of a climate-explicit  
208 matrix projection model (MPMs) structured by the discrete state variables size (number  
209 of tillers) and sex. The female-dominant and two-sex versions of the model both allow  
210 for sex-specific response to climate and differ only in the feedback between operational  
211 sex ratio and seed fertilization. For clarity of presentation we do not explicitly include  
212 climate-dependence in the notation below, but the following model was evaluated over  
213 variation in seasonal temperature and precipitation.

Let  $F_{x,t}$  and  $M_{x,t}$  be the number of female and male plants of size  $x$  in year  $t$ , where  $x \in [1, \dots, U]$ . The minimum possible size is one tiller and  $U$  is the 95th percentile of observed maximum size (35 tillers). Let  $F_t^R$  and  $M_t^R$  be new female and male recruits in year  $t$ , which we treat as distinct from the rest of the size distribution because we assume they do not reproduce in their first year, consistent with our observations. For a pre-breeding census,

the expected numbers of recruits in year  $t+1$  is given by:

$$F_{t+1}^R = \sum_1^U [p^F(x) \cdot c^F(x) \cdot d \cdot v(\mathbf{F}_t, \mathbf{M}_t) \cdot m \cdot \rho] F_{x,t} \quad (1)$$

$$M_{t+1}^R = \sum_1^U [p^F(x) \cdot c^F(x) \cdot d \cdot v(\mathbf{F}_t, \mathbf{M}_t) \cdot m \cdot (1-\rho)] F_{x,t} \quad (2)$$

where  $p^F$  and  $c^F$  are flowering probability and panicle production for females of size  $x$ ,  $d$  is the number of seeds per female panicle,  $v$  is the probability that a seed is fertilized,  $m$  is the probability that a fertilized seed germinates, and  $\rho$  is the primary sex ratio (proportion of recruits that are female), which we assume to be 0.5 (Miller and Compagnoni, 2022b).

In the two-sex model, seed fertilization is a function of population structure, allowing for feedback between vital rates and operational sex ratio (OSR). In the context of the model, OSR is defined as the fraction of panicles that are female and is derived from the  $U \times 1$  vectors  $\mathbf{F}_t$  and  $\mathbf{M}_t$ :

$$v(\mathbf{F}_t, \mathbf{M}_t) = v_0 * \left[ 1 - \left( \frac{\sum_1^U p^F(x, z) c^F(x, z) F_{x,t}}{\sum_1^U p^F(x, z) c^F(x, z) F_{x,t} + p^M(x, z) c^M(x, z) M_{x,t}} \right)^\alpha \right] \quad (3)$$

The summations tally the total number of female and male panicles over the size distribution, giving the fraction of total panicles that are female. We focus on the female fraction of panicles and not female fraction of reproductive individuals because panicle number can vary widely depending on size; we assume that few males with many panicles vs. many males with few panicles are interchangeable pollination environments. Eq. 3 has the properties that seed fertilization is maximized at  $v_0$  as OSR approaches 100% male, goes to zero as OSR approaches 100% female, and parameter  $\alpha$  controls how female seed viability declines as male panicles become rare. We estimated these parameters using data from a sex ratio manipulation experiment, conducted in the center of the range, in which seed fertilization was measured in plots of varying OSR; this experiment is described elsewhere (Compagnoni et al., 2017) and is summarized in [Supplementary Method S.2.3](#)<sup>3</sup>. This experiment also provided estimates for seed number per panicle ( $d$ ) and germination rate ( $m$ ). Lacking data on climate-dependence, we assume that seed fertilization, seed number, and germination rate do not vary with climate.

---

<sup>3</sup>I think the supplement should also include a data figure showing the fit of the model to the experimental data.

The dynamics of the size-structured component of the population are given by:

$$F_{y,t+1} = [\sigma \cdot g^F(y, x=1)] F_t^R + \sum_L^U [s^F(x) \cdot g^F(y, x)] F_{x,t} \quad (4)$$

$$M_{y,t+1} = [\sigma \cdot g^M(y, x=1)] M_t^R + \sum_L^U [s^M(x) \cdot g^M(y, x)] M_{x,t} \quad (5)$$

231 The first terms indicate recruits that survived their first year and enter the size distribution  
 232 of established plants. We estimated the seedling survival probability  $\sigma$  using demographic  
 233 data from the congeneric species *Poa autumnalis* in east Texas (T.E.X. Miller and J.A. Rudgers,  
 234 *unpublished data*), and we assume that  $\sigma$  is the same across sexes and climatic variables. We did  
 235 this because we had little information on the early life cycle transitions of greenhouse-raised  
 236 transplants. We used  $g(y, x=1)$  (the future size distribution of one-tiller plants from the  
 237 transplant experiment) to give the probability that a surviving recruit reaches size  $y$ . The  
 238 second component of the equations indicates survival and size transition of established  
 239 plants from the previous year, where  $s$  and  $g$  give the probabilities of surviving at size  $x$  and  
 240 growing from sizes  $x$  to  $y$ , respectively, and superscripts indicate that these functions may  
 241 be unique to females ( $F$ ) and males ( $M$ ).

242 The model described above yields a  $2(U+1) \times 2(U+1)$  transition matrix. We estimated  
 243 the population growth rate  $\lambda$  of the female dominant model as the leading eigenvalue of  
 244 the transition matrix. Since the two-sex MPM is nonlinear (matrix elements affect and are  
 245 affected by population structure) we estimated  $\lambda$  and stable sex ratio (female fraction of all  
 246 individuals) and operational sex ratio (female fraction of panicles) by numerical simulation.  
 247 Since all parameters were estimated using MCMC sampling, we were able to propagate the  
 248 uncertainty in our estimates of the vital rate parameters to uncertainty in  $\lambda$ . Furthermore,  
 249 by sampling over distributions associated with site, block, and source population variance  
 250 terms, we are able to incorporate process error into the total uncertainty in  $\lambda$ , in addition  
 251 to the uncertainty that arises from imperfect knowledge of the parameter values. For example,  
 252 sampling over site and block variances accounts for regional and local spatial heterogeneity  
 253 that is not explained by climate, and sampling over source population variance accounts for  
 254 genetically-based demographic differences across the species' range.

## 255 Life Table Response Experiments

256 We conducted two types of Life Table Response Experiments (LTRE) to isolate contributions of  
 257 climate variables and sex-specific vital rates to variation in  $\lambda$ . First, to identify which aspect of  
 258 climate is most important for population viability, we used an LTRE based on a nonparametric

model for the dependence of  $\lambda$  on parameters associated with seasonal temperature and precipitation (Ellner et al., 2016). To do so, we used the RandomForest package to fit a regression model with four climatic variables (temperature of growing season, precipitation of growing season, temperature of the dormant season and precipitation of the dormant season) as predictors and  $\lambda$  calculated from the two sex model as response (Liaw et al., 2002). The regression model allowed the estimation of the relative importance of each predictor.

Second, to understand how climate drivers influence  $\lambda$  via sex-specific demography, we decomposed the effect of each climate variable on population growth rate ( $\lambda$ ) into contribution arising from the effect on each female and male vital rate using a “regression design” LTRE (Caswell, 1989, 2000). This LTRE decomposes the sensitivity of  $\lambda$  to climate according to:

$$\frac{\partial \lambda}{\partial \text{climate}} \approx \sum_i \frac{\partial \lambda}{\partial \theta_i^F} \frac{\partial \theta_i^F}{\partial \text{climate}} + \frac{\partial \lambda}{\partial \theta_i^M} \frac{\partial \theta_i^M}{\partial \text{climate}} \quad (6)$$

where,  $\theta_i^F$  and  $\theta_i^M$  represent sex-specific parameters (the regression coefficients of the vital rate functions). Because LTRE contributions are additive, we summed across vital rates to compare the total contributions of female and male parameters.<sup>45</sup>

## Population viability across the climatic niche and geographic range

To understand how climate shapes the niche and geographic range of Texas bluegrass, we estimated the probability of self-sustaining populations ( $\Pr(\lambda \geq 1)$ ) conditional to temperature and precipitation of the dormant and growing seasons.  $\Pr(\lambda > 1)$  was calculated for the two-sex model and the female dominant MPMs using the proportion of the 300 posterior samples that lead to a  $\lambda \geq 1$  (Diez et al., 2014). Population viability in climate niche space was then represented as a contour plot with values of  $\Pr(\lambda > 1)$  at given temperature and precipitation for the growing season, holding dormant season climate constant, and vice versa.

$\Pr(\lambda > 1)$  was also mapped onto geographic layers of three US states (Texas, Oklahoma and Kansas) to delineate past, current and future potential geographic distribution of the species. To do so, we estimated  $\Pr(\lambda > 1)$  conditional to all climate covariates for each pixel ( $\sim 25 \text{ km}^2$ ) for each time period (past, present, future). Because of the amount of the computation involved, we use 100 posterior samples to estimate  $\Pr(\lambda > 1)$  across the study area (Texas, Oklahoma and Kansas).

---

<sup>4</sup>Let's talk about this

<sup>5</sup>I do not agree. It is true that you can compute this, but only by “turning off” the interaction by holding the interacting variable constant. I still think this needs to be better addressed in both LTRE analyses.

286 **Results**

287 **Sex specific demographic responses and sex ratio variation across climatic  
288 conditions**

289 We found strong demographic responses to climate drivers across our Texas bluegrass  
290 common garden sites and years, and evidence for demographic differences between the  
291 sexes. Regression coefficients related to sex and/or sex:size interactions were significantly  
292 non-zero (95% credible intervals excluding zero) for most vital rates (Fig. S-4), suggesting  
293 sexual divergence in demography. Females generally had an advantage over males, especially  
294 in survival and flowering (Fig. 2). **Across all sites and years, % of females survived compared  
295 to % of males, and % of surviving females flowered compared to % of surviving males.**<sup>6</sup>  
296 Furthermore, there were significant interactions between sex and one or more climate  
297 variables, particularly for growth (Fig. S-4B), indicating sexual niche divergence in response  
298 to shared climate drivers. Figures S-5 and S-6 visualize the magnitude of sexual divergence  
299 in demography across niche space, revealing that female advantages in flowering and panicle  
300 production were greatest at both high and low growing season temperature extremes.

---

<sup>6</sup>*I think it would be interesting to add just the raw numbers here.*

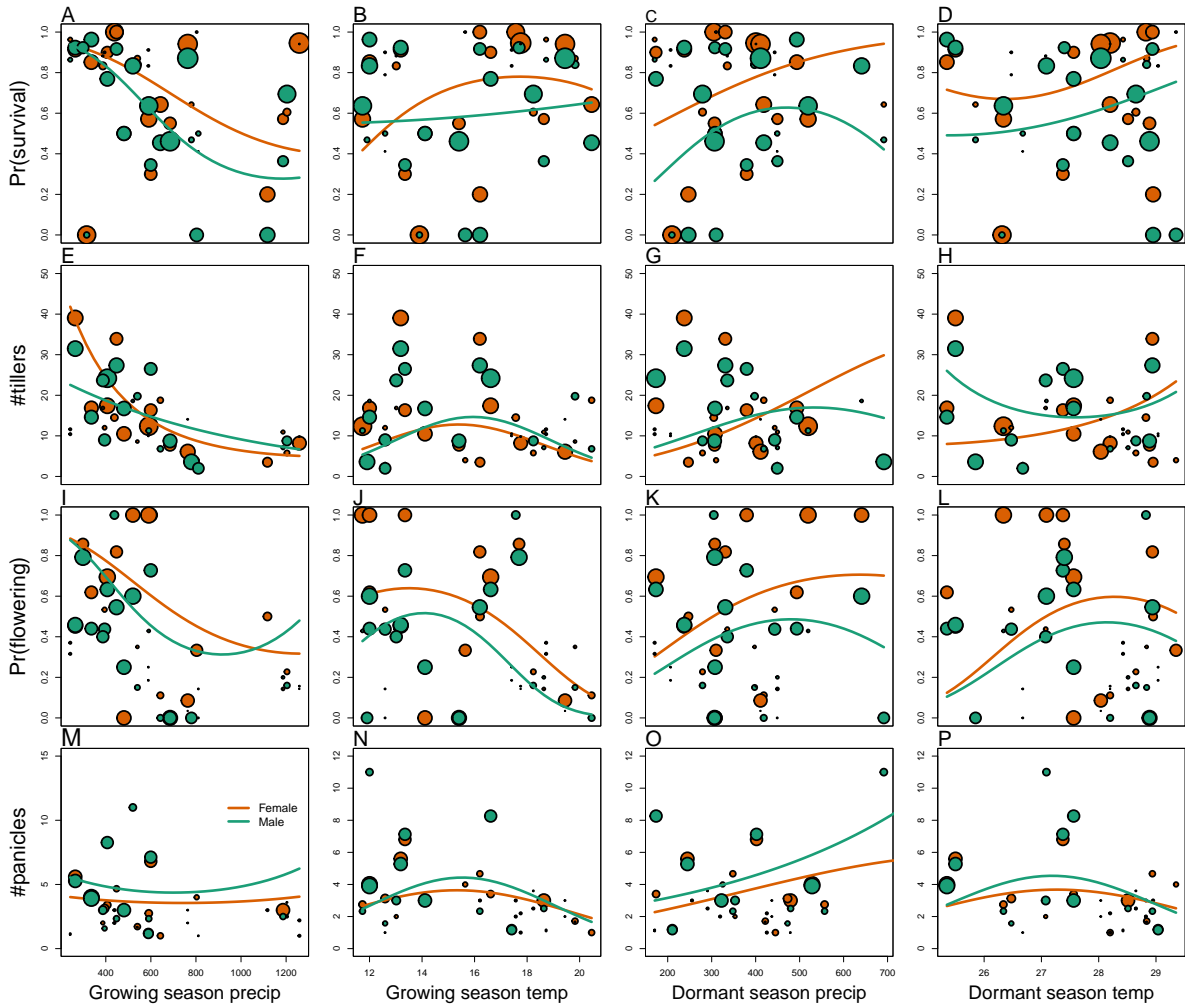


**Figure 2: Sex specific demographic response to climate across species range.** (A, B, C, D) Probability of survival as a function of precipitation and temperature of the growing and dormant season. (E, F, G, H) Change in number of tillers as a function of precipitation and temperature of the growing and dormant season. (I, J, K, L) Probability of flowering as a function of precipitation and temperature of growing and dormant season. (M, N, O, P) Change in number of panicles as a function of precipitation and temperature of the growing and dormant season. Points show means by site for females (orange) and males (green). Points sizes are proportional to the sample sizes of the mean and are jittered. Lines show fitted statistical models for females (orange) and males (green) based on posterior mean parameter values.

301 Across common garden sites, operational sex ratio (proportion of panicles that are female)  
 302 of the experimental populations was female-biased on average ( $\approx 60\%$  female), reflecting the  
 303 overall greater rates of female vs. male flowering rather than bias in the underlying population  
 304 composition. OSR was most female-biased (up to 80% female) at extreme values of tempera-  
 305 ture, especially growing season temperature (Figure S-7, Figure S-8), consistent with the female  
 306 reproductive advantage at temperature extremes seen in the vital rate data (Figure S-5). In  
 307 contrast, there was very little variation in sex ratio (proportion of plants that are female) in the

308 years following common garden establishment (all sites were planted with equal numbers of fe-  
309 males and males) and no detectable influence of climate covariates (Figure S-9), indicating that  
310 skew in the OSR comes from sex-biased reproductive rates more so than sex-biased survival.

### 311 Climate drivers of population viability across niche space

312 Putting all vital rates together in the MPM framework reveals how climate shapes fitness  
313 variation across niche dimensions and geographic space, and how accounting for sex structure  
314 modifies these inferences. Figure 3 shows the estimated probability of population viability  
315 ( $\lambda \geq 1$ ) across seasonal climate niche space; these probabilities account for uncertainty in the  
316 vital rate parameters as well as process error related to spatial heterogeneity and genotypic  
317 variation. For both female-dominant and two-sex models, fitness variation across niche space  
318 was dominated by temperature, with weaker effects of precipitation (compare vertical and  
319 horizontal contours in Fig. 3). These visual trends are supported by LTRE decomposition  
320 indicating that variation in fitness across climatic conditions is most strongly driven by  
321 responses to growing and dormant season temperature, with weaker interactive effects of  
322 precipitation that modulate the effects of temperature (Figure S-11). LTRE analysis also showed  
323 that declines in population viability at high and low temperatures were driven most strongly  
324 by reductions in vegetative growth and panicle production, with stronger contributions from  
325 females than males (Figure S-12). Intermediate temperatures of both growing and dormant  
326 seasons were associated with near-certain projections of population viability ( $Pr(\lambda \geq 1) \approx 1$ ),  
327 and high and low temperature extremes during both seasons were associated with low niche  
328 suitability ( $Pr(\lambda \geq 1) < 0.2$ ). Higher precipitation slightly expanded the range of suitable  
329 temperatures during the dormant season (Fig. 3A), and the reverse was true in the growing  
330 season (Fig. 3B). Points in Fig. 3 show that climate change forecasted for the common  
331 garden locations would move many of them toward lower-suitability regions of niche space  
332 associated with high growing and dormant season temperatures (see also Fig. S-13).

333 While the female-dominant and two-sex models were generally in agreement about high  
334 confidence in intermediate temperature optima, they differed around the edges of niche space  
335 (Fig. 3C,D,S-13). The female-dominant model over-predicted population viability, especially  
336 with respect to growing season temperature. For example, the female-dominant model  
337 predicted<sup>7</sup> that, for most levels of precipitation, warm growing season (winter) temperatures  
338 of  $\sim 20^{\circ}\text{C}$  had high suitability ( $Pr(\lambda \geq 1) > 0.9$ ), while the two-sex model indicated that these  
339 conditions were most likely unsuitable ( $Pr(\lambda \geq 1) < 0.5$ ). Similarly, at low winter temperatures  
340 that the two-sex model identifies with high certainty as unsuitable ( $Pr(\lambda \geq 1) < 0.1$ ), the

---

<sup>7</sup> I think I am switching tenses. We will need to clean this up.

341 female-dominant model is more optimistic ( $Pr(\lambda \geq 1) > 0.4$ ). Across growing season climate  
342 space, the female-dominant model over-estimates population viability by ca. 10%, on average  
343 (Fig. 3D, Fig. S-15B). The difference between female-dominant and two-sex models was  
344 qualitatively similar but weaker in magnitude for niche dimensions of the dormant season  
345 (Fig. 3C, Fig. S-15A).<sup>8</sup> Female-dominant and two-sex models diverged most strongly in  
346 regions of niche space that favored strongly female-biased operational sex ratios (Figure  
347 S-16)<sup>910</sup>. This suggests mate limitation as the biological mechanism underlying model  
348 differences. The two-sex model accounts for feedbacks between OSR and female fertility, with  
349 reduced seed viability at OSR exceeding ~ 75% female panicles (Fig. WE NEED A FIGURE  
350 FOR THIS)<sup>1112</sup>. Lacking this feedback, the female-dominant model over-predicts population  
351 viability in regions of niche space where male flowering is not sufficient to maximize seed set.

---

<sup>8</sup>The niche histogram figure is duplicated in the supplement. Also, can you add a legend to this figure?

<sup>9</sup>This Figure is new and I am not sure if we should keep it in the manuscript

<sup>10</sup>I like it!

<sup>11</sup>I don't understand the type of Figure you are asking here

<sup>12</sup>I am talking about a figure showing how seed viability declines with increasing female bias in the OSR.

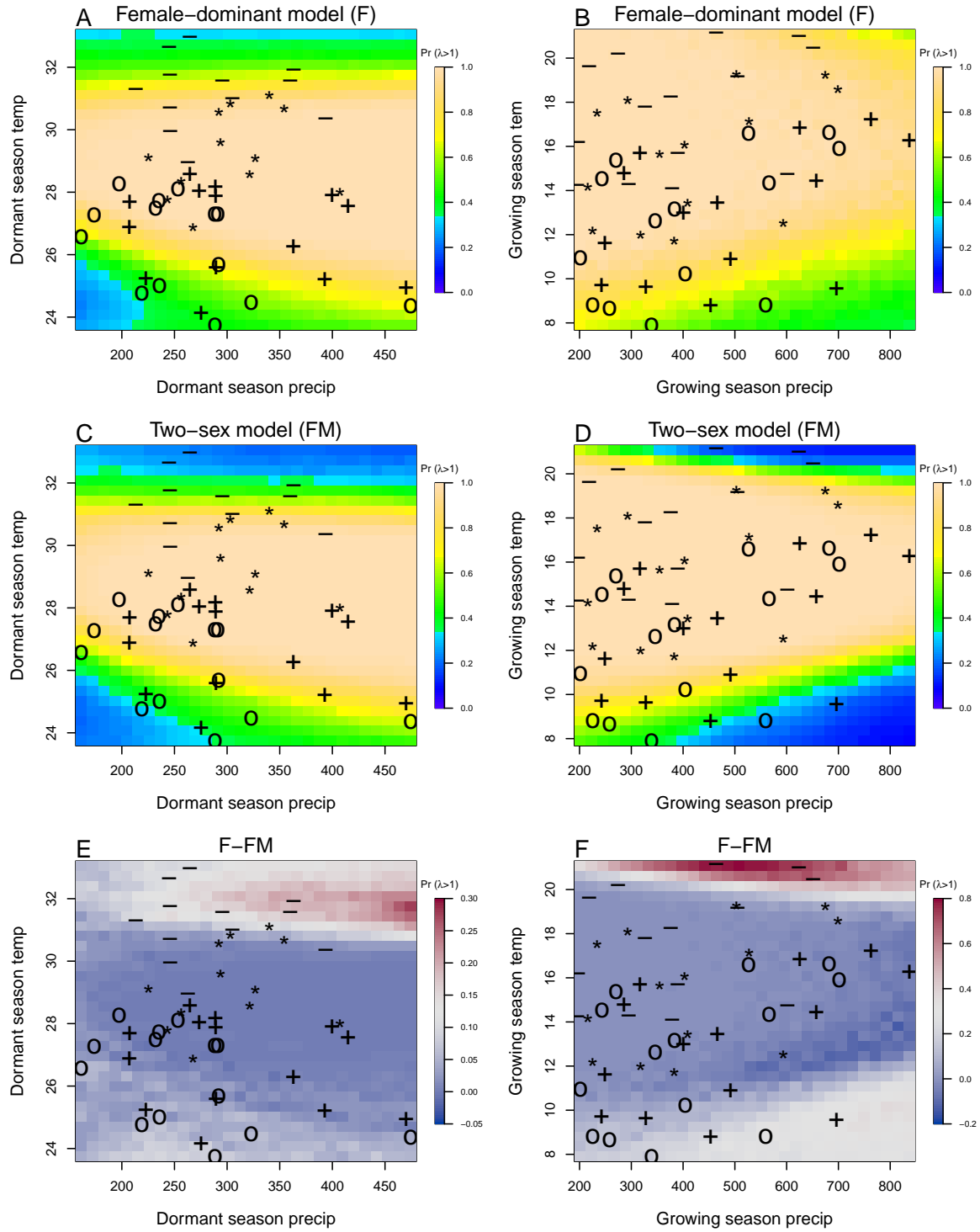


**Figure 3: A two-dimensional representation of the predicted niche shift over time (past, present and future climate conditions). "O": Past, "+" Current, "\*": RCP 4.5, "-": RCP 8.5.**

352 **Climatic change induces shifts in geographic niche and population OSR**

353 Projecting the climatic niche onto geographic space, we find that suitable niche conditions for  
354 Texas bluegrass are shifting north under climate change (Fig. 4). Under past (1901-1930) and  
355 present (1990-2019) conditions, the two-sex and female-dominant models predict widespread  
356 suitability with high confidence ( $Pr(\lambda \geq 1) \approx 1$ ) across much of Texas and Oklahoma. For  
357 both models, the predicted geographic niche generally corresponds well to independent  
358 observations of the Texas bluegrass distribution (Fig. 4). The predicted geographic niche is  
359 more expansive than the observed distribution, particularly at southern, western, and eastern  
360 edges, suggesting some degree of range disequilibrium (e.g., due to dispersal limitation),  
361 geographic bias in occurrence observations, and/or model mis-specification. Comparing past  
362 to present conditions, the geographic niche for both models has shifted slightly poleward,  
363 with reductions in viability at the southern margins and expansions of viability at northern  
364 margins. The northward shift of suitable niche conditions is even more pronounced in  
365 projections to end-of-century (2071-2100) conditions, with the most dramatic changes in the  
366 most pessimistic (RCP8.5) scenario (Fig. 4.<sup>13</sup>). In fact, under the pessimistic scenario, Texas  
367 bluegrass will have very little remaining climate suitability in the state of Texas by the end  
368 of the 21st century. The predicted poleward niche shift is consistent across different global  
369 circulation models (Figure S-17, Figure S-18, Figure S-19).

370 Female-dominant and two-sex models are in broad agreement about northward migration  
371 of the climatic niche, but the geographic projections reveal hotspots of disagreement where the  
372 female-dominant model over-predicts climate suitability and under-predicts the likelihood of  
373 range shifts (Fig. 4). These hotspots are generally regions of predicted female bias in the oper-  
374 ational sex ratio (Figure 6) The strongest contrast between the two models is in the pessimistic  
375 climate change scenario (RCP8.5), where the female-dominant model over-predicts population  
376 viability by ca. 25%<sup>14</sup> across much of the region (Figure S-20) and under-estimates the mag-  
377 nitude of a potential range shift. In this scenario, a broad swath of the current distribution  
378 that is forecasted to be effectively unsuitable ( $Pr(\lambda \geq 1) \approx 0$ ) by the two-sex model is identified  
379 as marginally suitable ( $Pr(\lambda \geq 1) \approx 0.5$ ) by the female-dominant model. Accordingly, the OSR  
380 of Texas bluegrass across its range is projected to be ca. 75% female panicles, on average, by  
381 end of century under RCP8.5, an increase from ca. 60% female under projections for past and  
382 current conditions (Fig. 5). The more optimistic climate change scenario (RCP4.5) predicts  
383 an intermediate shift in OSR, with hotspots of change becoming strongly female-biased but  
384 most of the range remaining near current levels of 60% female (Fig. 5; Fig. 6).

---

<sup>13</sup>I am not sure if we need a title for each panel.

<sup>14</sup>I just eyeballed this. Real number should come from the histograms.

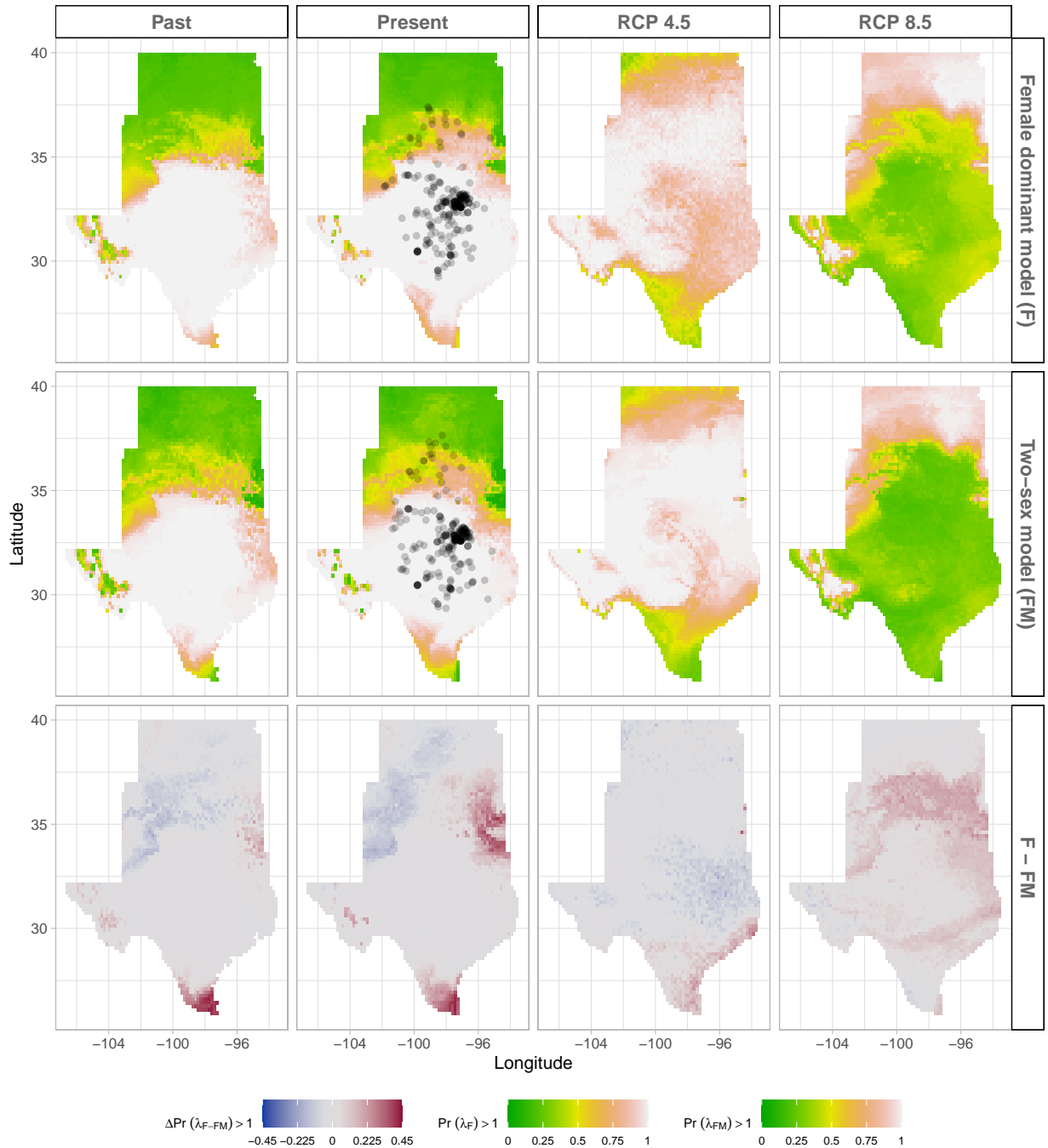


**Figure 4: Climate change favors range shift towards north edge.** (A) Past, (B) Current, (C and D) Future predicted range shift based on the predicted probabilities of self- sustaining populations,  $\text{Pr}(\lambda > 1)$ , using the two-sex model that incorporates sex- specific demographic responses to climate with sex ratio dependent seed fertilization. (E) Past, (F) Current, (G and H) Future predicted range shift based on the predicted probabilities of self- sustaining populations,  $\text{Pr}(\lambda > 1)$ , using the female dominant model. Future projections were based on the CMCC-CM model. The black dots on panel B and F indicate all known presence points collected from GBIF. The occurrences of GBIFs are distributed in with higher population fitness habitat  $\text{Pr}(\lambda > 1)$  , confirming that our study approach can reasonably predict range shifts.

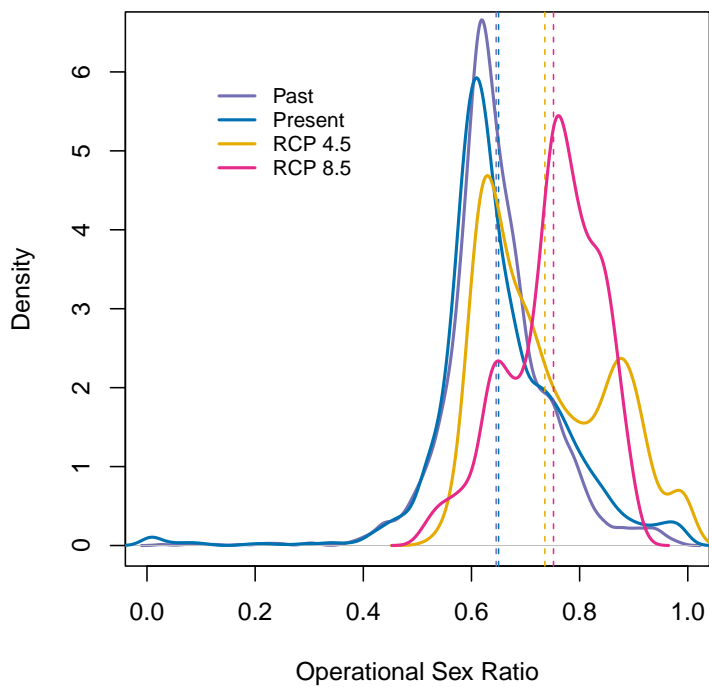


**Figure 5:** Change in Operational Sex Ratio (proportion of female panicle) over time (past, present, future). Future projections were based on the CMCC-CM model. The mean sex ratio for each time period is shown as vertical dashed line.

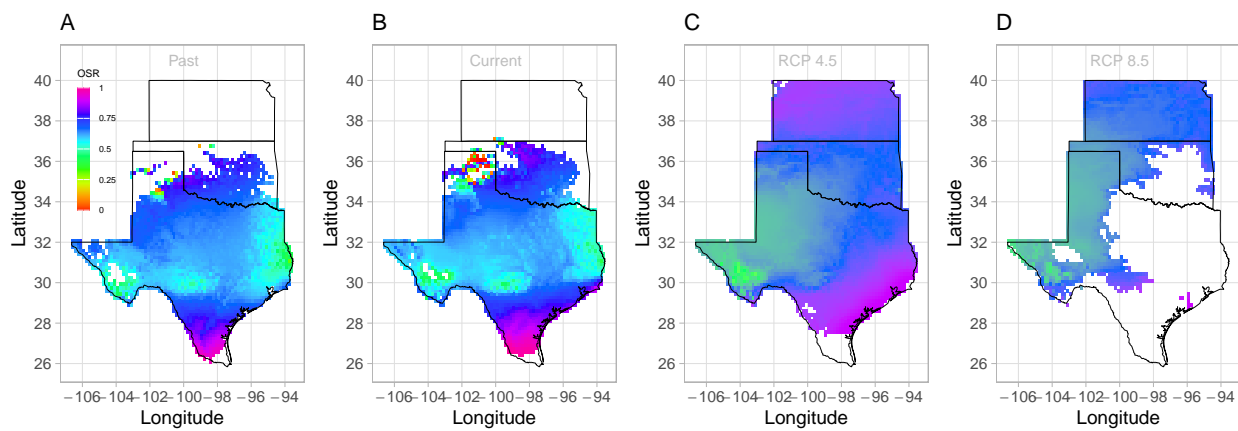


**Figure 6:** Change in Operational Sex Ratio (proportion of female panicle) over time (past, present, future) across species range. Future projections were based on the CMCC-CM model. The mean sex ratio for each time period is shown as vertical dashed line.

385 **Discussion**

386 Dioecious species make up a large fraction of Earth's biodiversity – most animals and many  
387 plants – yet we have little knowledge about how sex-specific demography and responses to  
388 climate drivers may affect population viability and range shifts of dioecious species under  
389 climate change.<sup>15</sup> We used demographic data collected common garden experiments and  
390 sex-structured demographic modeling to forecast for the first time the likely impact of climate  
391 change on range dynamics of a dioecious species. Our future projections require extrapolation  
392 to warmer or colder conditions than observed in our experiment and subsequently should be  
393 interpreted with caution (Chen et al., 2024).<sup>16</sup> Three general patterns emerged from our analysis  
394 of range-wide common garden experiments and sex-structured, climate-explicit demographic  
395 models. First, our Bayesian mixed effect model suggests a sex specific demographic response  
396 to climate change that lead to higher proportion of female as climate increase. Second, climate  
397 change favors a northern range shifts in suitable habitats. Third, the female dominant model  
398 (model that does not account for sex structure) overestimates species niche and range shifts.

399 There was a female demographic advantage leading to a female biased in response  
400 to climate change in *Poa arachnifera* populations. The extreme female-bias in response to  
401 climate change contrast with previous studies suggesting that an increase in male frequency  
402 in response to climate change (Hultine et al., 2016; Petry et al., 2016). Two mechanisms  
403 could explain the observed demographic advantage of females over males for survival and  
404 flowering and the opposite for growth and number of panicles. The trade-off between fitness  
405 traits (survival, growth and fertility) due to resource limitation and the pollination mode of  
406 our study species (wind pollinated) could explain such a result (Cipollini and Whigham, 1994;  
407 Freeman et al., 1976). For most species, the cost of reproduction is often higher for females  
408 than males due to the requirement to develop seeds and fruits (Hultine et al., 2016). However,  
409 several studies reported a higher cost of reproduction for males in wind pollinated species  
410 due to the larger amounts of pollen they produce (Bruijning et al., 2017; Bürli et al., 2022;  
411 Cipollini and Whigham, 1994; Field et al., 2013).

412 Our results suggest that climate change will alter population at the center of the range  
413 and drive a northern range shifts. This impact of climate change on the species current  
414 niche could be explained by the increase of temperature over the next years. Small change  
415 in temperature of the growing and dormant season have a larger impact on population  
416 viability. Temperature can impact plant populations through different mechanisms. Increasing  
417 temperature could increase evaporative demand, affect plant phenology (Iler et al., 2019;

---

<sup>15</sup>Love this opening sentence.

<sup>16</sup>I think extrapolation should be its own paragraph. This also relates to uncertainty in the climate forecasts.

418 McLean et al., 2016; Sherry et al., 2007), and germination rate (Reed et al., 2021). The potential  
419 for temperature to influence these different processes changes seasonally (Konapala et al.,  
420 2020). For example, studies suggested that species that are active during the growing season  
421 such as cool grass species can have delayed phenology in response to global warming,  
422 particularly if temperatures rise above their physiological tolerances (Cleland et al., 2007;  
423 Williams et al., 2015). In addition, high temperature during the growing season by affecting  
424 pollen viability, fertilization could affect seed formation and germination (Hatfield and  
425 Prueger, 2015; Sletvold and Ågren, 2015). Pollen dispersal may allow plants to resist climate  
426 change because pollen dispersal may provide the local genetic diversity necessary to adapt  
427 at the leading edge of the population (Corlett and Westcott, 2013; Duputié et al., 2012; Kremer  
428 et al., 2012). Since wind pollination is most effective at short distances, it is most often  
429 found in plant species growing at high density such as our study species, it is less likely  
430 that dispersal limitation affect niche shift in our study system. Difference in non-climatic  
431 factors such as soil, or biotic interactions could also explain decline in population growth rate  
432 as an indirect effects of increase in temperature (Alexander et al., 2015; Schultz et al., 2022).  
433 For example, climate change could increase the strength of species competition and thereby  
434 constrain our study species to a narrower realized niche (Aguilée et al., 2016; Pulliam, 2000).

435 We found evidence of underestimation of the impact of climatic change on population  
436 dynamics by the female dominant model and implication for such an underestimation on  
437 conservation actions for dioecious species. The underestimation of the impact of climatic  
438 change on population dynamics by the female dominant model makes sense given the sex  
439 specific response to climatic change. *Poa arachnifera* populations will be female biased in  
440 response to climate change. That extreme female-bias could affect population growth rate  
441 by altering males' fitness with reduction on mate availability given that females individuals  
442 have a demographic advantage over males (Haridas et al., 2014; Knight et al., 2005). Further,  
443 our work suggest that population viability is sensitive to climate under current and future  
444 conditions. This is key because most conservation actions are design from data on current  
445 responses to climate, rather than future response to climate (Sletvold et al., 2013). Since the  
446 role of male is not negligible in accuralrtly predicting dioecious species response to climate  
447 change, management strategies that focus on both sexes would be effective and will enhance  
448 our understanding of dioecious species response to global warming.

## 449 Conclusion

450 We have investigated the potential consequence of skewness in sex ratio on population  
451 dynamics and range shift in the context of climate change using the Texas bluegrass. We

452 found extreme female -biased in response to climate change. The effect of female biased  
453 will induce range shifts to the northern edge of the species current range by limiting mate  
454 availability. Beyond, our study case, our results also suggest that tracking only one sex could  
455 lead to an underestimation of the effect of climate change on population dynamics. Our  
456 work provides also a framework for predicting the impact of global warming on population  
457 dynamics using the probability of population to self-sustain.

458 **Acknowledgements**

459 This research was supported by National Science Foundation Division of Environmental  
460 Biology awards 2208857 and 2225027. We thank the institutions who hosted us at their field  
461 station facilities, including

462 **References**

- 463 Aguilée, R., Raoul, G., Rousset, F., and Ronce, O. (2016). Pollen dispersal slows geographical  
464 range shift and accelerates ecological niche shift under climate change. *Proceedings of the  
465 National Academy of Sciences*, 113(39):E5741–E5748.
- 466 Alexander, J. M., Diez, J. M., and Levine, J. M. (2015). Novel competitors shape species'  
467 responses to climate change. *Nature*, 525(7570):515–518.
- 468 Bertrand, R., Lenoir, J., Piedallu, C., Riofrío-Dillon, G., De Ruffray, P., Vidal, C., Pierrat, J.-C.,  
469 and Gégout, J.-C. (2011). Changes in plant community composition lag behind climate  
470 warming in lowland forests. *Nature*, 479(7374):517–520.
- 471 Bruijning, M., Visser, M. D., Muller-Landau, H. C., Wright, S. J., Comita, L. S., Hubbell, S. P.,  
472 de Kroon, H., and Jongejans, E. (2017). Surviving in a cosexual world: A cost-benefit  
473 analysis of dioecy in tropical trees. *The American Naturalist*, 189(3):297–314.
- 474 Bürli, S., Pannell, J. R., and Tonnabel, J. (2022). Environmental variation in sex ratios and  
475 sexual dimorphism in three wind-pollinated dioecious plant species. *Oikos*, 2022(6):e08651.
- 476 Caswell, H. (1989). Analysis of life table response experiments i. decomposition of effects  
477 on population growth rate. *Ecological Modelling*, 46(3-4):221–237.
- 478 Caswell, H. (2000). *Matrix population models*, volume 1. Sinauer Sunderland, MA.
- 479 Chen, X., Liang, Y., and Feng, X. (2024). Influence of model complexity, training collinearity,  
480 collinearity shift, predictor novelty and their interactions on ecological forecasting. *Global  
481 Ecology and Biogeography*, 33(3):371–384.
- 482 Cipollini, M. L. and Whigham, D. F. (1994). Sexual dimorphism and cost of reproduction  
483 in the dioecious shrub *lindera benzoin* (lauraceae). *American Journal of Botany*, 81(1):65–75.
- 484 Cleland, E. E., Chuine, I., Menzel, A., Mooney, H. A., and Schwartz, M. D. (2007). Shifting  
485 plant phenology in response to global change. *Trends in ecology & evolution*, 22(7):357–365.
- 486 Compagnoni, A., Steigman, K., and Miller, T. E. (2017). Can't live with them, can't live  
487 without them? balancing mating and competition in two-sex populations. *Proceedings of  
488 the Royal Society B: Biological Sciences*, 284(1865):20171999.
- 489 Corlett, R. T. and Westcott, D. A. (2013). Will plant movements keep up with climate change?  
490 *Trends in ecology & evolution*, 28(8):482–488.

- 491 Czachura, K. and Miller, T. E. (2020). Demographic back-casting reveals that subtle  
492 dimensions of climate change have strong effects on population viability. *Journal of Ecology*,  
493 108(6):2557–2570.
- 494 Dahlgren, J. P., Bengtsson, K., and Ehrlén, J. (2016). The demography of climate-driven and  
495 density-regulated population dynamics in a perennial plant. *Ecology*, 97(4):899–907.
- 496 Davis, M. B. and Shaw, R. G. (2001). Range shifts and adaptive responses to quaternary  
497 climate change. *Science*, 292(5517):673–679.
- 498 Diez, J. M., Giladi, I., Warren, R., and Pulliam, H. R. (2014). Probabilistic and spatially variable  
499 niches inferred from demography. *Journal of ecology*, 102(2):544–554.
- 500 Duputié, A., Massol, F., Chuine, I., Kirkpatrick, M., and Ronce, O. (2012). How do genetic cor-  
501 relations affect species range shifts in a changing environment? *Ecology letters*, 15(3):251–259.
- 502 Eberhart-Phillips, L. J., Küpper, C., Miller, T. E., Cruz-López, M., Maher, K. H., Dos Remedios,  
503 N., Stoffel, M. A., Hoffman, J. I., Krüger, O., and Székely, T. (2017). Sex-specific early  
504 survival drives adult sex ratio bias in snowy plovers and impacts mating system and  
505 population growth. *Proceedings of the National Academy of Sciences*, 114(27):E5474–E5481.
- 506 Ehrlén, J. and Morris, W. F. (2015). Predicting changes in the distribution and abundance  
507 of species under environmental change. *Ecology letters*, 18(3):303–314.
- 508 Elderd, B. D. and Miller, T. E. (2016). Quantifying demographic uncertainty: Bayesian methods  
509 for integral projection models. *Ecological Monographs*, 86(1):125–144.
- 510 Ellis, R. P., Davison, W., Queirós, A. M., Kroeker, K. J., Calosi, P., Dupont, S., Spicer, J. I.,  
511 Wilson, R. W., Widdicombe, S., and Urbina, M. A. (2017). Does sex really matter? explaining  
512 intraspecies variation in ocean acidification responses. *Biology letters*, 13(2):20160761.
- 513 Ellner, S. P., Adler, P. B., Childs, D. Z., Hooker, G., Miller, T. E., and Rees, M. (2022). A critical  
514 comparison of integral projection and matrix projection models for demographic analysis:  
515 Comment. *Ecology*.
- 516 Ellner, S. P., Childs, D. Z., Rees, M., et al. (2016). Data-driven modelling of structured  
517 populations. *A practical guide to the Integral Projection Model*. Cham: Springer.
- 518 Evans, M. E., Merow, C., Record, S., McMahon, S. M., and Enquist, B. J. (2016). Towards  
519 process-based range modeling of many species. *Trends in Ecology & Evolution*, 31(11):860–871.

- 520 Field, D. L., Pickup, M., and Barrett, S. C. (2013). Comparative analyses of sex-ratio variation  
521 in dioecious flowering plants. *Evolution*, 67(3):661–672.
- 522 Freeman, D. C., Klikoff, L. G., and Harper, K. T. (1976). Differential resource utilization by  
523 the sexes of dioecious plants. *Science*, 193(4253):597–599.
- 524 Gamelon, M., Grøtan, V., Nilsson, A. L., Engen, S., Hurrell, J. W., Jerstad, K., Phillips, A. S.,  
525 Røstad, O. W., Slagsvold, T., Walseng, B., et al. (2017). Interactions between demography  
526 and environmental effects are important determinants of population dynamics. *Science  
527 Advances*, 3(2):e1602298.
- 528 Gerber, L. R. and White, E. R. (2014). Two-sex matrix models in assessing population viability:  
529 when do male dynamics matter? *Journal of Applied Ecology*, 51(1):270–278.
- 530 Gissi, E., Bowyer, R. T., and Bleich, V. C. (2024). Sex-based differences affect conservation.  
531 *Science*, 384(6702):1309–1310.
- 532 Gissi, E., Schiebinger, L., Hadly, E. A., Crowder, L. B., Santoleri, R., and Micheli, F. (2023).  
533 Exploring climate-induced sex-based differences in aquatic and terrestrial ecosystems to  
534 mitigate biodiversity loss. *nature communications*, 14(1):4787.
- 535 Haridas, C., Eager, E. A., Rebarber, R., and Tenhumberg, B. (2014). Frequency-dependent  
536 population dynamics: Effect of sex ratio and mating system on the elasticity of population  
537 growth rate. *Theoretical Population Biology*, 97:49–56.
- 538 Hatfield, J. and Prueger, J. (2015). Temperature extremes: effect on plant growth and  
539 development. *weather clim extrem* 10: 4–10.
- 540 Hernández, C. M., Ellner, S. P., Adler, P. B., Hooker, G., and Snyder, R. E. (2023). An exact  
541 version of life table response experiment analysis, and the r package exactltre. *Methods  
542 in Ecology and Evolution*, 14(3):939–951.
- 543 Hitchcock, A. S. (1971). *Manual of the grasses of the United States*, volume 2. Courier Corporation.
- 544 Hultine, K. R., Grady, K. C., Wood, T. E., Shuster, S. M., Stella, J. C., and Whitham, T. G. (2016).  
545 Climate change perils for dioecious plant species. *Nature Plants*, 2(8):1–8.
- 546 Iler, A. M., Compagnoni, A., Inouye, D. W., Williams, J. L., CaraDonna, P. J., Anderson, A., and  
547 Miller, T. E. (2019). Reproductive losses due to climate change-induced earlier flowering are  
548 not the primary threat to plant population viability in a perennial herb. *Journal of Ecology*,  
549 107(4):1931–1943.

- 550 Jones, M. H., Macdonald, S. E., and Henry, G. H. (1999). Sex-and habitat-specific responses  
551 of a high arctic willow, *salix arctica*, to experimental climate change. *Oikos*, pages 129–138.
- 552 Karger, D. N., Conrad, O., Böhner, J., Kawohl, T., Kreft, H., Soria-Auza, R. W., Zimmermann,  
553 N. E., Linder, H. P., and Kessler, M. (2017). Climatologies at high resolution for the earth's  
554 land surface areas. *Scientific data*, 4(1):1–20.
- 555 Kindiger, B. (2004). Interspecific hybrids of *poa arachnifera* × *poa secunda*. *Journal of New  
556 Seeds*, 6(1):1–26.
- 557 Knight, T. M., Steets, J. A., Vamosi, J. C., Mazer, S. J., Burd, M., Campbell, D. R., Dudash,  
558 M. R., Johnston, M. O., Mitchell, R. J., and Ashman, T.-L. (2005). Pollen limitation of plant  
559 reproduction: pattern and process. *Annu. Rev. Ecol. Evol. Syst.*, 36:467–497.
- 560 Konapala, G., Mishra, A. K., Wada, Y., and Mann, M. E. (2020). Climate change will affect  
561 global water availability through compounding changes in seasonal precipitation and  
562 evaporation. *Nature communications*, 11(1):3044.
- 563 Kremer, A., Ronce, O., Robledo-Arnuncio, J. J., Guillaume, F., Bohrer, G., Nathan, R., Bridle,  
564 J. R., Gomulkiewicz, R., Klein, E. K., Ritland, K., et al. (2012). Long-distance gene flow and  
565 adaptation of forest trees to rapid climate change. *Ecology letters*, 15(4):378–392.
- 566 Lee-Yaw, J. A., Kharouba, H. M., Bontrager, M., Mahony, C., Csergő, A. M., Noreen, A. M.,  
567 Li, Q., Schuster, R., and Angert, A. L. (2016). A synthesis of transplant experiments and  
568 ecological niche models suggests that range limits are often niche limits. *Ecology letters*,  
569 19(6):710–722.
- 570 Liaw, A., Wiener, M., et al. (2002). Classification and regression by randomforest. *R news*,  
571 2(3):18–22.
- 572 Louthan, A. M., Keighron, M., Kiekebusch, E., Cayton, H., Terando, A., and Morris, W. F.  
573 (2022). Climate change weakens the impact of disturbance interval on the growth rate of  
574 natural populations of venus flytrap. *Ecological Monographs*, 92(4):e1528.
- 575 Lynch, H. J., Rhainds, M., Calabrese, J. M., Cantrell, S., Cosner, C., and Fagan, W. F. (2014).  
576 How climate extremes—not means—define a species' geographic range boundary via a  
577 demographic tipping point. *Ecological Monographs*, 84(1):131–149.
- 578 McLean, N., Lawson, C. R., Leech, D. I., and van de Pol, M. (2016). Predicting when climate-  
579 driven phenotypic change affects population dynamics. *Ecology Letters*, 19(6):595–608.

- 580 Merow, C., Bois, S. T., Allen, J. M., Xie, Y., and Silander Jr, J. A. (2017). Climate change both  
581 facilitates and inhibits invasive plant ranges in new england. *Proceedings of the National*  
582 *Academy of Sciences*, 114(16):E3276–E3284.
- 583 Miller, T. and Compagnoni, A. (2022a). Data from: Two-sex demography, sexual niche  
584 differentiation, and the geographic range limits of texas bluegrass (*Poa arachnifera*). *American*  
585 *Naturalist, Dryad Digital Repository*,. <https://doi.org/10.5061/dryad.kkwh70s5x>.
- 586 Miller, T. E. and Compagnoni, A. (2022b). Two-sex demography, sexual niche differentiation,  
587 and the geographic range limits of texas bluegrass (*poa arachnifera*). *The American*  
588 *Naturalist*, 200(1):17–31.
- 589 Miller, T. E., Shaw, A. K., Inouye, B. D., and Neubert, M. G. (2011). Sex-biased dispersal and  
590 the speed of two-sex invasions. *The American Naturalist*, 177(5):549–561.
- 591 Morrison, C. A., Robinson, R. A., Clark, J. A., and Gill, J. A. (2016). Causes and consequences  
592 of spatial variation in sex ratios in a declining bird species. *Journal of Animal Ecology*,  
593 85(5):1298–1306.
- 594 Pease, C. M., Lande, R., and Bull, J. (1989). A model of population growth, dispersal and  
595 evolution in a changing environment. *Ecology*, 70(6):1657–1664.
- 596 Petry, W. K., Soule, J. D., Iler, A. M., Chicas-Mosier, A., Inouye, D. W., Miller, T. E., and  
597 Mooney, K. A. (2016). Sex-specific responses to climate change in plants alter population  
598 sex ratio and performance. *Science*, 353(6294):69–71.
- 599 Piironen, J. and Vehtari, A. (2017). Comparison of bayesian predictive methods for model  
600 selection. *Statistics and Computing*, 27:711–735.
- 601 Pottier, P., Burke, S., Drobniak, S. M., Lagisz, M., and Nakagawa, S. (2021). Sexual (in) equality?  
602 a meta-analysis of sex differences in thermal acclimation capacity across ectotherms.  
603 *Functional Ecology*, 35(12):2663–2678.
- 604 Pulliam, H. R. (2000). On the relationship between niche and distribution. *Ecology letters*,  
605 3(4):349–361.
- 606 R Core Team (2023). *R: A Language and Environment for Statistical Computing*. R Foundation  
607 for Statistical Computing, Vienna, Austria.
- 608 Reed, P. B., Peterson, M. L., Pfeifer-Meister, L. E., Morris, W. F., Doak, D. F., Roy, B. A., Johnson,  
609 B. R., Bailes, G. T., Nelson, A. A., and Bridgman, S. D. (2021). Climate manipulations

- 610 differentially affect plant population dynamics within versus beyond northern range limits.  
611 *Journal of Ecology*, 109(2):664–675.
- 612 Renganayaki, K., Jessup, R., Burson, B., Hussey, M., and Read, J. (2005). Identification of  
613 male-specific aflp markers in dioecious texas bluegrass. *Crop science*, 45(6):2529–2539.
- 614 Sanderson, B. M., Knutti, R., and Caldwell, P. (2015). A representative democracy to reduce  
615 interdependency in a multimodel ensemble. *Journal of Climate*, 28(13):5171–5194.
- 616 Schultz, E. L., Hülsmann, L., Pillet, M. D., Hartig, F., Breshears, D. D., Record, S., Shaw, J. D.,  
617 DeRose, R. J., Zuidema, P. A., and Evans, M. E. (2022). Climate-driven, but dynamic and  
618 complex? a reconciliation of competing hypotheses for species' distributions. *Ecology letters*,  
619 25(1):38–51.
- 620 Schwalm, C. R., Glendon, S., and Duffy, P. B. (2020). Rcp8. 5 tracks cumulative co2 emissions.  
621 *Proceedings of the National Academy of Sciences*, 117(33):19656–19657.
- 622 Schwinning, S., Lortie, C. J., Esque, T. C., and DeFalco, L. A. (2022). What common-garden  
623 experiments tell us about climate responses in plants.
- 624 Sexton, J. P., McIntyre, P. J., Angert, A. L., and Rice, K. J. (2009). Evolution and ecology of  
625 species range limits. *Annu. Rev. Ecol. Evol. Syst.*, 40:415–436.
- 626 Shelton, A. O. (2010). The ecological and evolutionary drivers of female-biased sex ratios:  
627 two-sex models of perennial seagrasses. *The American Naturalist*, 175(3):302–315.
- 628 Sherry, R. A., Zhou, X., Gu, S., Arnone III, J. A., Schimel, D. S., Verburg, P. S., Wallace,  
629 L. L., and Luo, Y. (2007). Divergence of reproductive phenology under climate warming.  
630 *Proceedings of the National Academy of Sciences*, 104(1):198–202.
- 631 Sletvold, N. and Ågren, J. (2015). Climate-dependent costs of reproduction: Survival and  
632 fecundity costs decline with length of the growing season and summer temperature.  
633 *Ecology Letters*, 18(4):357–364.
- 634 Sletvold, N., Dahlgren, J. P., Øien, D.-I., Moen, A., and Ehrlén, J. (2013). Climate warming  
635 alters effects of management on population viability of threatened species: results from  
636 a 30-year experimental study on a rare orchid. *Global Change Biology*, 19(9):2729–2738.
- 637 Smith, M. D., Wilkins, K. D., Holdrege, M. C., Wilfahrt, P., Collins, S. L., Knapp, A. K., Sala,  
638 O. E., Dukes, J. S., Phillips, R. P., Yahdjian, L., et al. (2024). Extreme drought impacts have  
639 been underestimated in grasslands and shrublands globally. *Proceedings of the National  
640 Academy of Sciences*, 121(4):e2309881120.

- 641 Stan Development Team (2023). RStan: the R interface to Stan. R package version 2.21.8.
- 642 Thomson, A. M., Calvin, K. V., Smith, S. J., Kyle, G. P., Volke, A., Patel, P., Delgado-Arias,  
643 S., Bond-Lamberty, B., Wise, M. A., Clarke, L. E., et al. (2011). Rcp4. 5: a pathway for  
644 stabilization of radiative forcing by 2100. *Climatic change*, 109:77–94.
- 645 Tognetti, R. (2012). Adaptation to climate change of dioecious plants: does gender balance  
646 matter? *Tree Physiology*, 32(11):1321–1324.
- 647 Williams, J. L., Jacquemyn, H., Ochocki, B. M., Brys, R., and Miller, T. E. (2015). Life  
648 history evolution under climate change and its influence on the population dynamics of  
649 a long-lived plant. *Journal of Ecology*, 103(4):798–808.

# Supporting Information

## 650 S.1 Supporting Figures

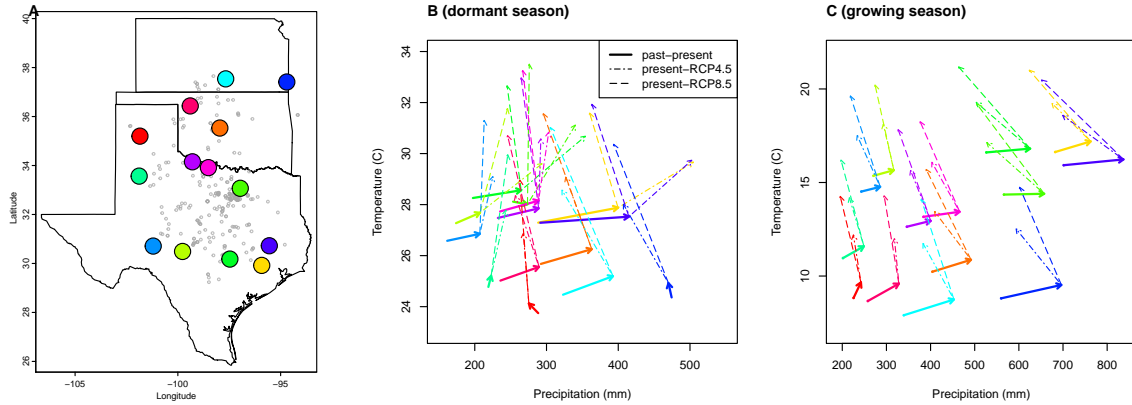


**Figure S-1:** (A), Common garden locations in Texas, Oklahoma, and Kansas (points) and (B,C) corresponding changes in growing and dormant season climate. Arrows in B,C connect past (1901-1930) and present (1990-2019) climate normals, and present and future (2071-2100) climate normals under RCP4.5 and RCP8.5 forecasts. Future forecasts are from MIROC5 but other climate models show similar patterns.

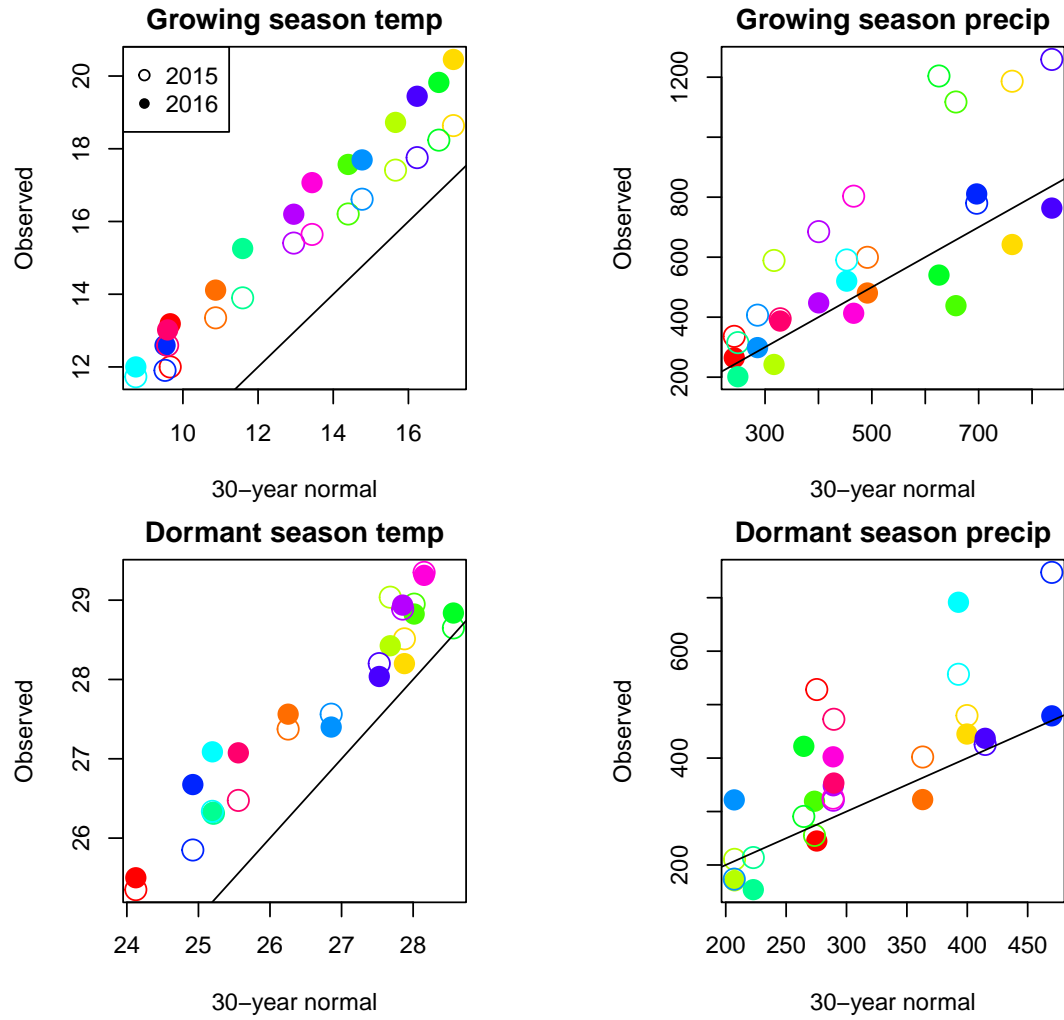


**Figure S-2:** Comparison of 30-year (1990-2019) climate normals and observed weather conditions at common garden sites during the 2014–15 and 2015–16 census periods. Temperature is in  $^{\circ}\text{C}$  and precipitation is in  $\text{mm}$ . Colors represent sites and lines show the  $y=x$  relationship.

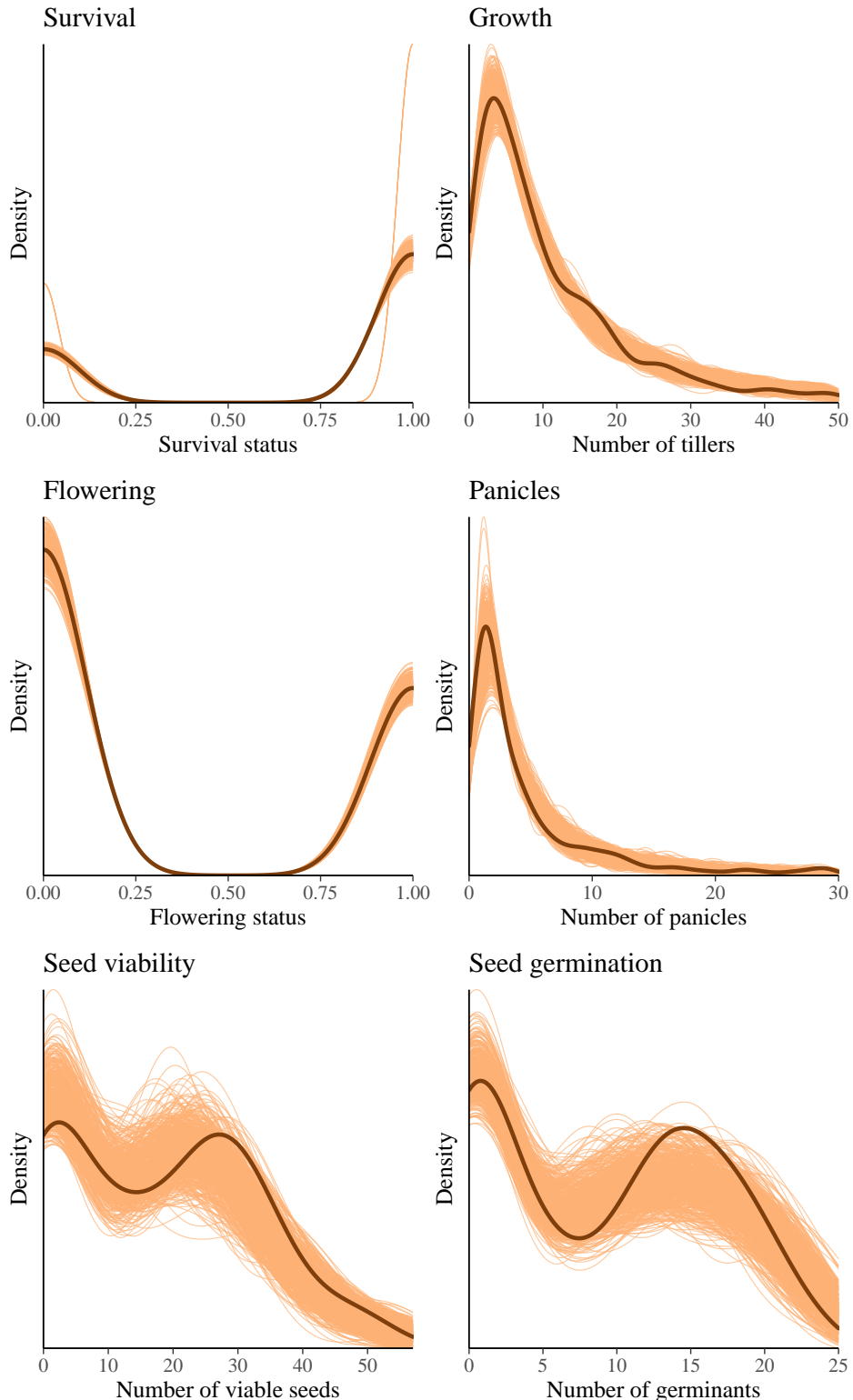


**Figure S-3:** Posterior predictive checks. Consistency between real data and simulated values suggests that the fitted vital rate models accurately describes the data. Graph shows density curves for the observed data (light orange) along with the simulated values (dark orange).

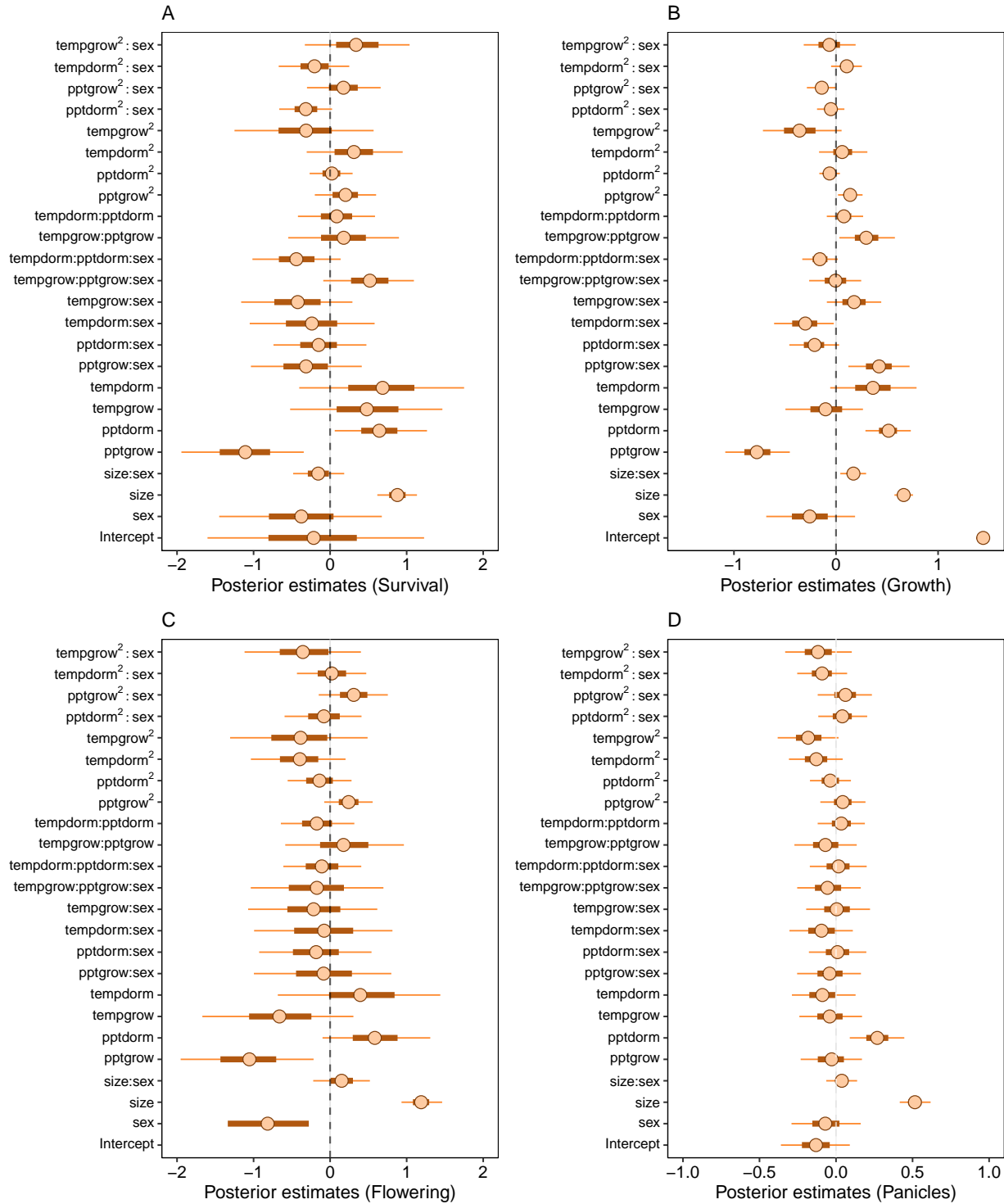


**Figure S-4:** Mean parameter values and 95% credible intervals of the posterior probability distributions. pptgrow is the precipitation of growing season, Tempgrow is the temperature of growing season, pptdorm is the temperature of dormant season, Tempdorm is the temperature of dormant season.

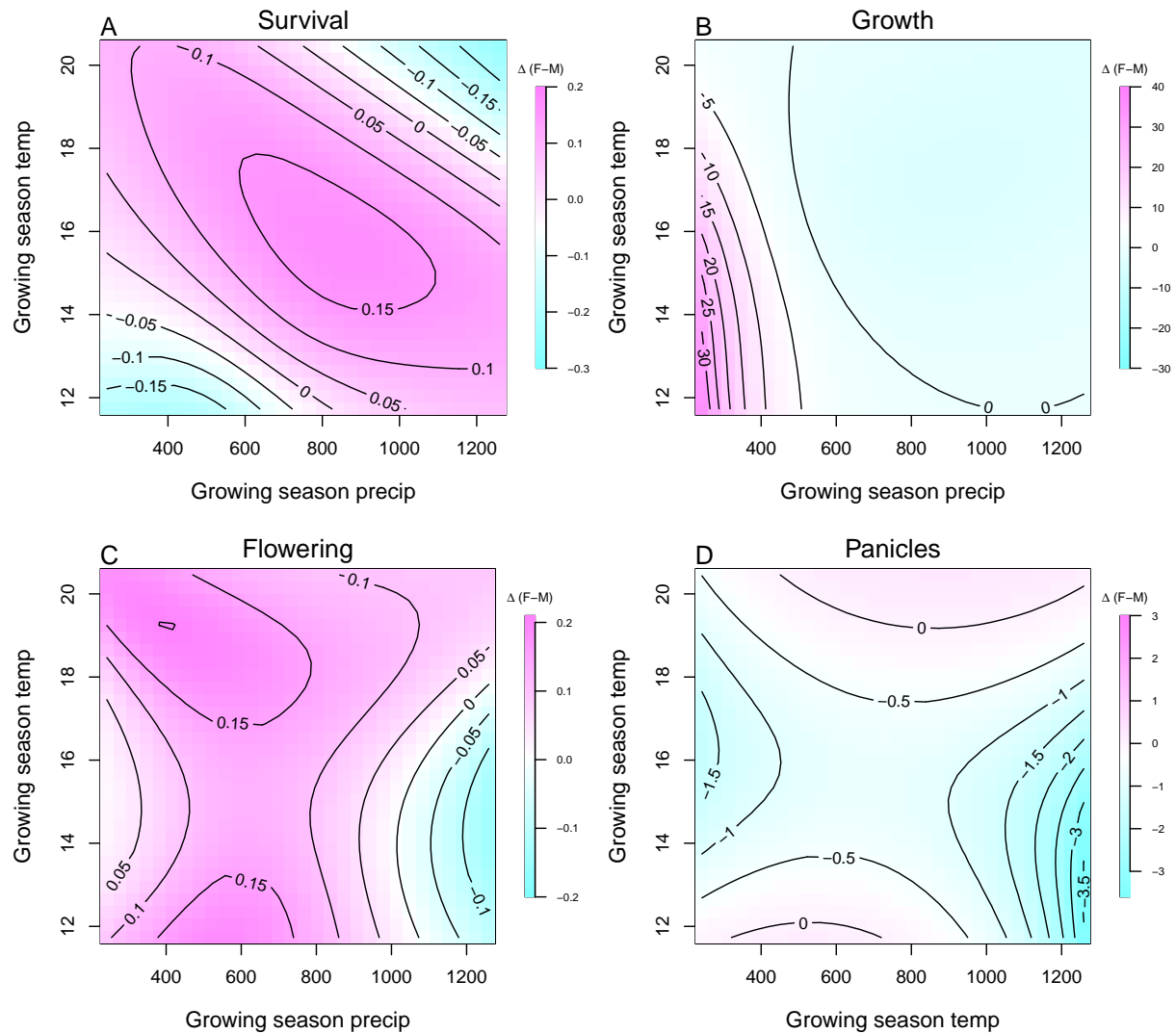


**Figure S-5:** Predicted difference in demographic response to climate across species range between female and male. Contours show predicted value of that difference conditional on precipitation and temperature of growing season

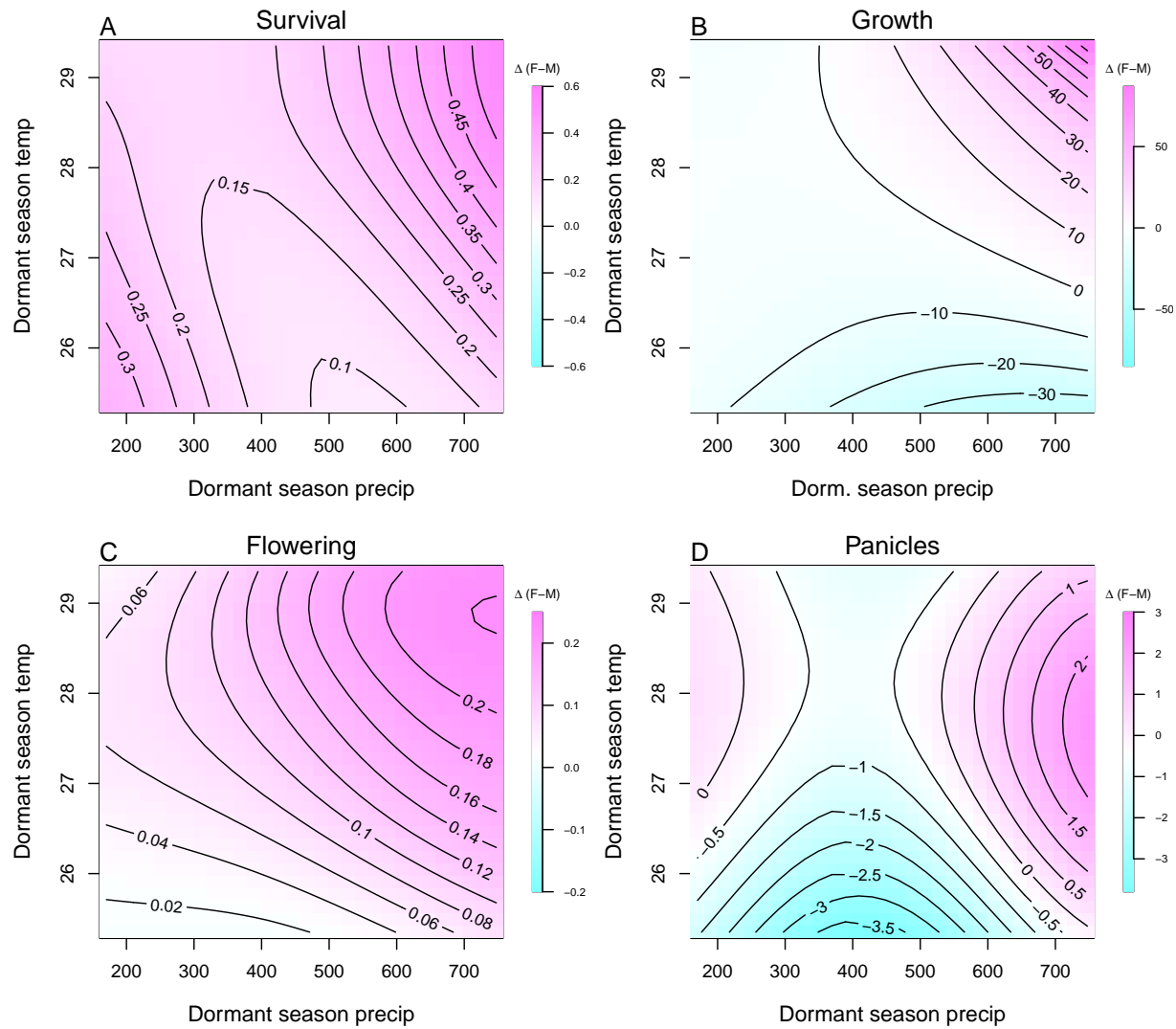


**Figure S-6:** Predicted difference in demographic response to climate across species range between female and male. Contours show predicted value of that difference conditional on precipitation and temperature of the dormant season

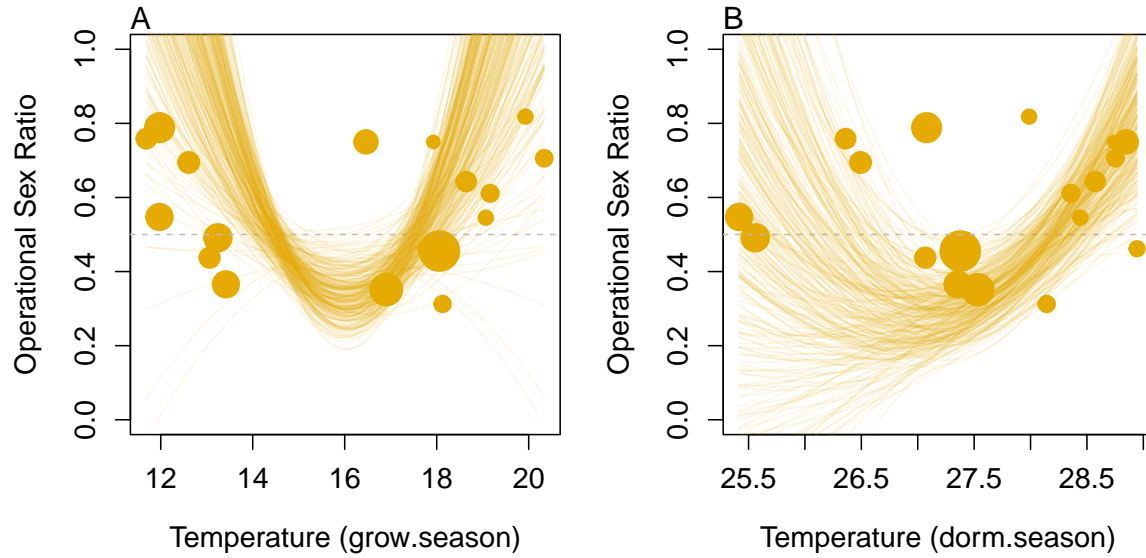


**Figure S-7: Significant Operational Sex Ratio response across climate gradient.** (A, B) Proportion of panicles that were females across temperature of the growing and dormant season

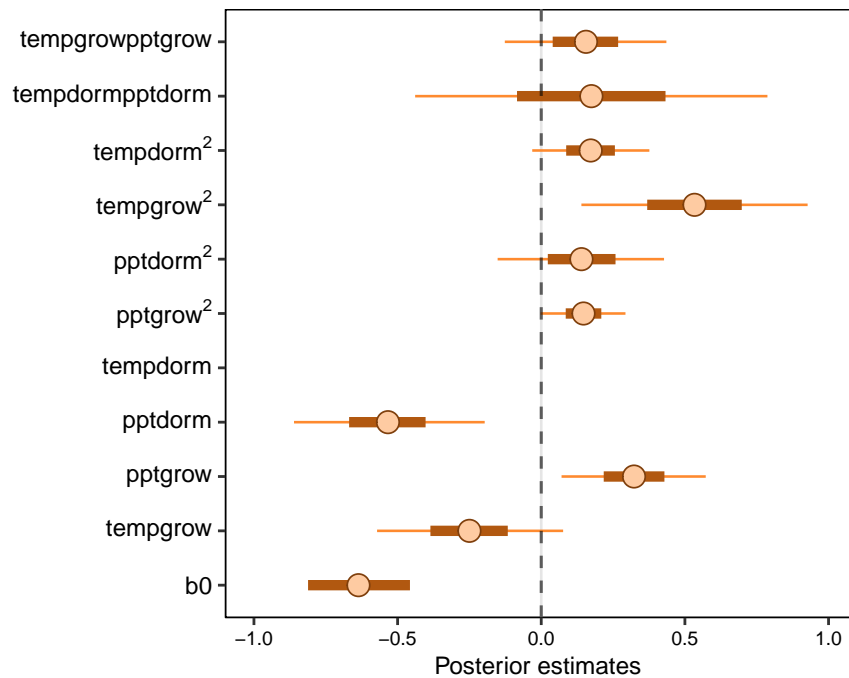


**Figure S-8:** Mean parameter values and 95% credible intervals of the posterior probability distributions for climate drivers of operational sex ratio (female fraction of total panicles) across common garden years and sites. pptgrow is the precipitation of growing season, Tempgrow is the temperature of growing season, pptdorm is the temperature of dormant season, Tempdorm is the temperature of dorm. season.

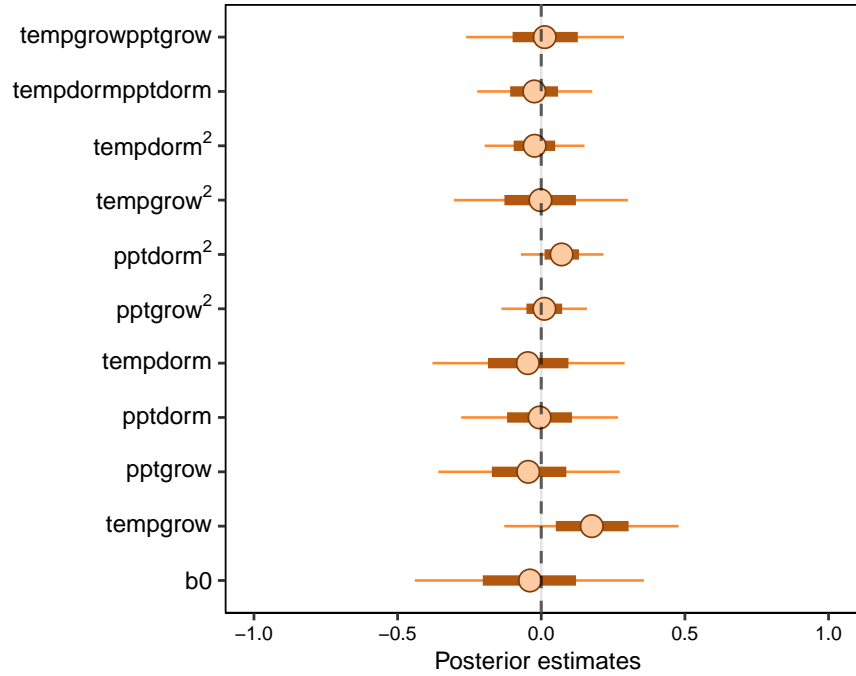


**Figure S-9:** Mean parameter values and 95% credible intervals of the posterior probability distributions for climate drivers of sex ratio (female fraction of the populations) across common garden years and sites. pptgrow is the precipitation of growing season, Tempgrow is the temperature of growing season, pptdorm is the temperature of dormant season, Tempdorm is the temperature of dormant season.

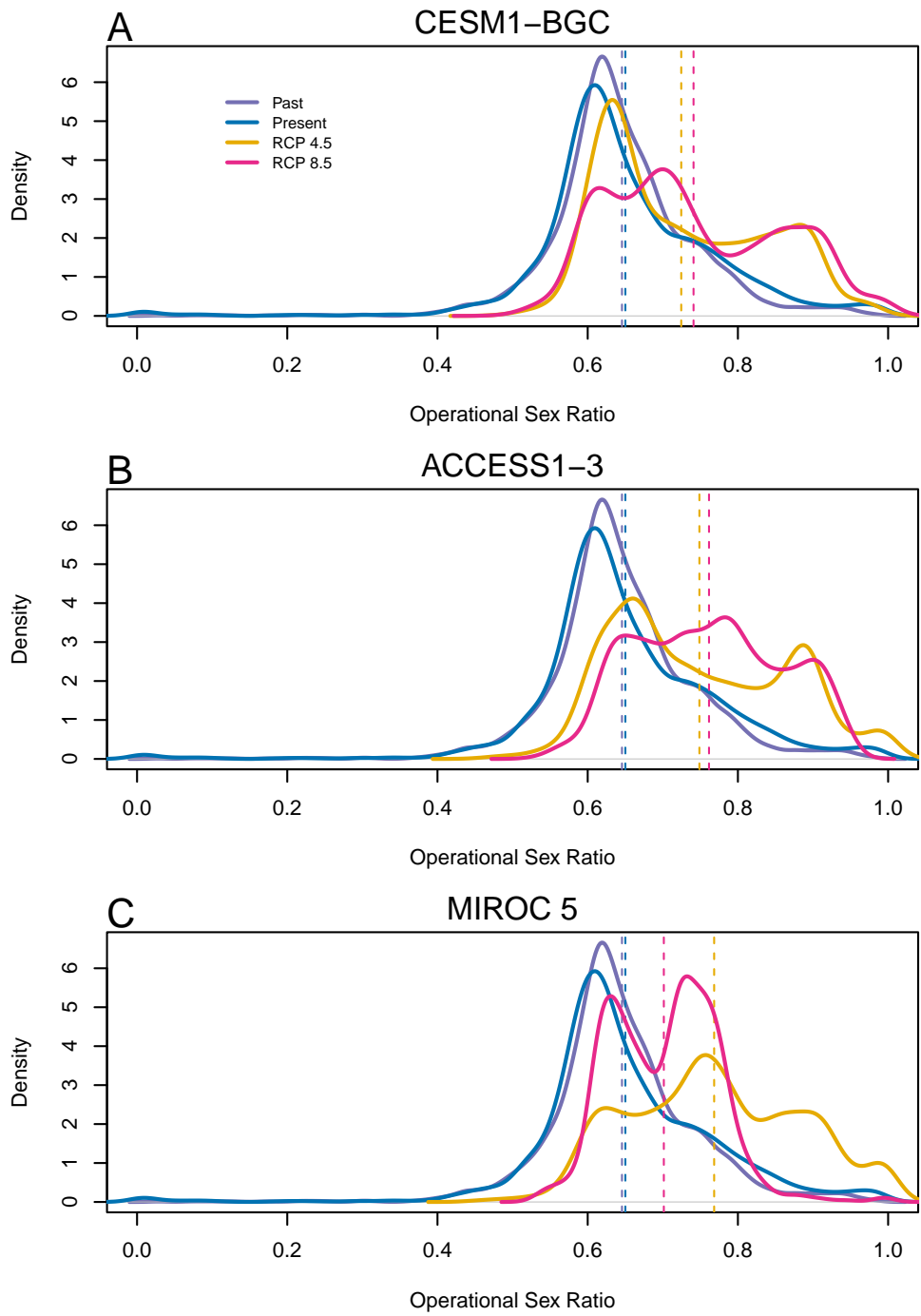


**Figure S-10:** Change in Operational Sex Ratio (proportion of female) over time (past, present, future). Future projections were based on A) MIROC 5, B) CES, C) ACC. The means for each model are shown as vertical dashed lines.

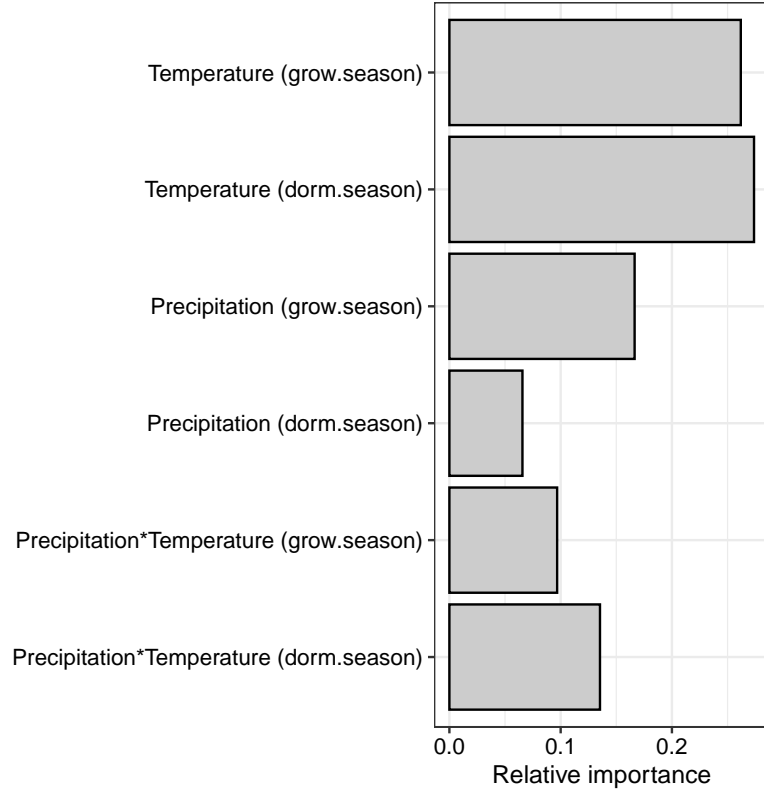


**Figure S-11:** Life Table Response Experiment: The bar represent the relative importance of each predictors.

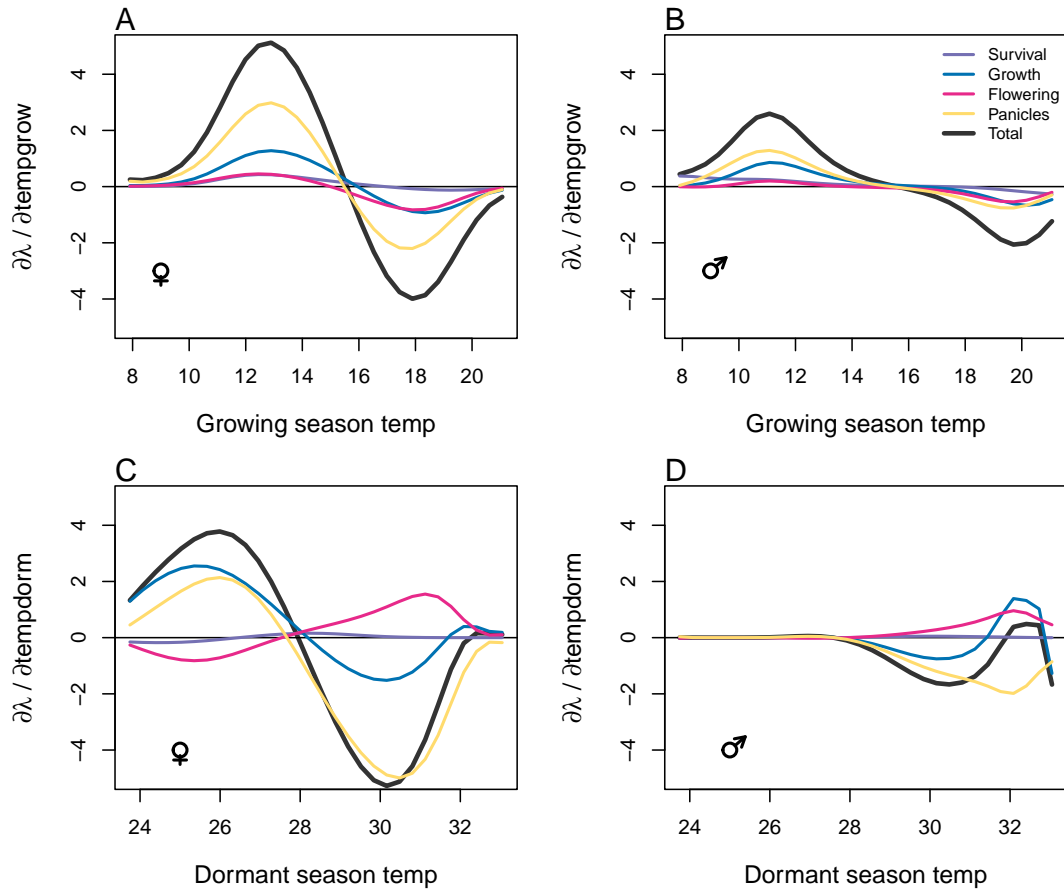


**Figure S-12:** Life table response experiment decomposition of the sensitivity of  $\lambda$  to seasonal climate into additive vital rate contributions of males and females based on posterior mean parameter estimates. (A) Temperature of growing season (contribution of female), (B) Temperature of growing season (contribution of male), (C) Temperature of dormant season (contribution of female) and (D) Temperature of dormant season (contribution of male).

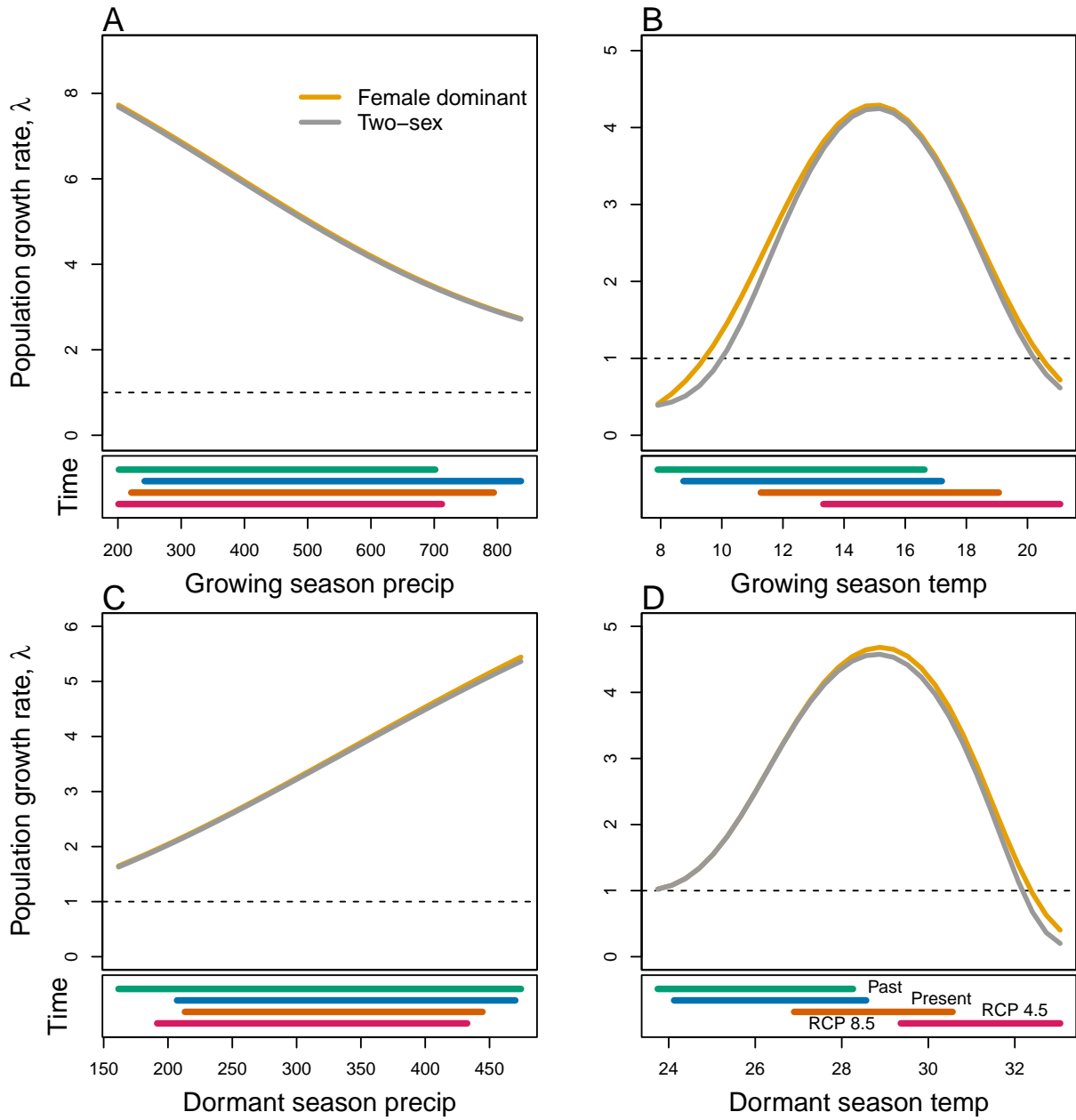


**Figure S-13: Predicted population growth rate ( $\lambda$ ) in different ranges of climate.** (A) Precipitation of the growing season, (B) Temperature of the growing season, (C) Precipitation of the dormant season, (D) Temperature of the dormant season. The grey curve shows prediction by the two-sex matrix projection model that incorporates sex-specific demographic responses to climate with sex ratio dependent seed fertilization. The orange curve represents the prediction by the female dominant matrix projection model. The dashed horizontal line indicates the limit of population viability ( $\lambda = 1$ ). Lower panels below each data panel show ranges of climate values for different time period (past climate, present and future climates). For future climate, we show a Representation Concentration Pathways (RCP) 4.5 and 8.5. Values population viability of ( $\lambda$ ) are derived from the mean climate variables across 4 GCMs (MIROC5, ACCESS1-3, CESM1-BGC, CMCC-CM).

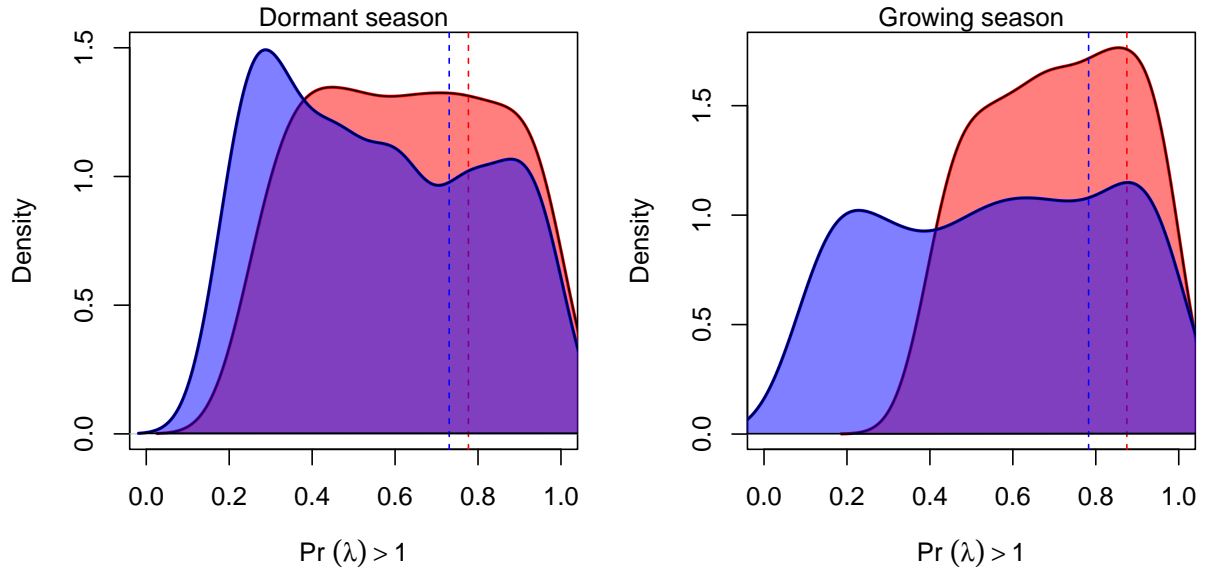


**Figure S-14:** Assessment of the statistical difference between the two-sex models and the female dominant model for the dormant and growing season. Plots show the density of  $\text{Pr}(\lambda > 1)$  values for female dominant (pink) and two-sex models (violet) for each season. The means for each model are shown as vertical dashed lines.

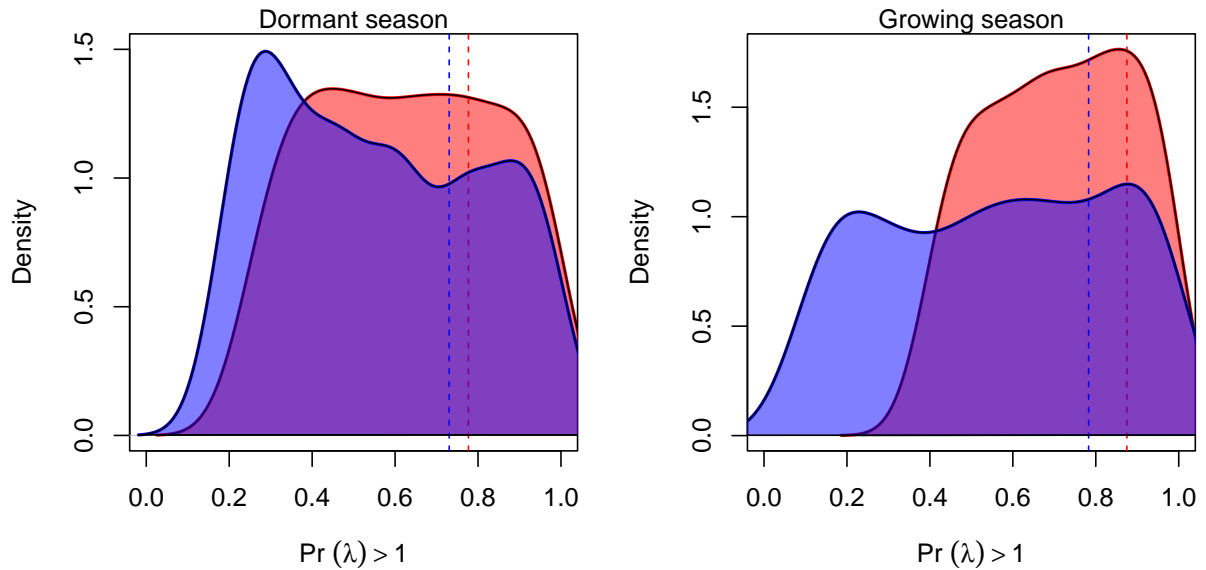


**Figure S-15:** Assessment of the statistical difference between the two-sex models and the female dominant model for the dormant and growing season. Plots show the density of  $\text{Pr}(\lambda > 1)$  values for female dominant (pink) and two-sex models (violet) for each season. The means for each model are shown as vertical dashed lines.

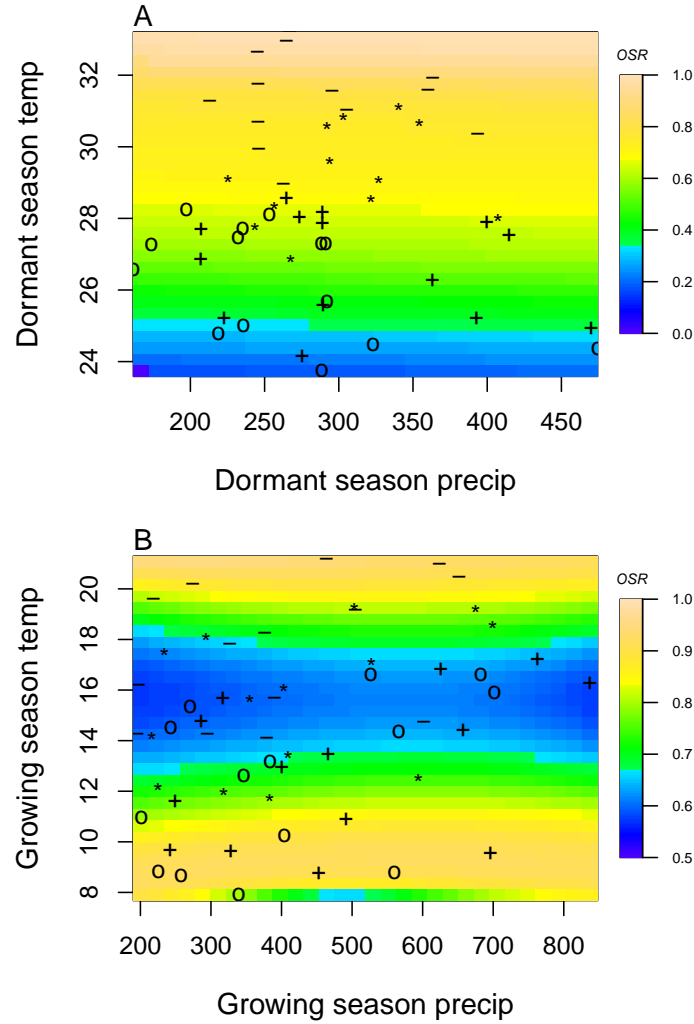


**Figure S-16:** A two-dimensional representation of the Operational Sex Ratio (OSR) over time (past, present and future climate conditions). OSR represents the proportion of females. Contours show predicted values of OSR conditional on precipitation and temperature of the dormant and growing season. Operational Sex Ratio during the dormant season for the two sex model (A), Operational Sex Ratio during the growing season for the two sex model (B). “**o**”: Past, “**+**”: Current, “**\***”: RCP 4.5, “**-**”: RCP 8.5.

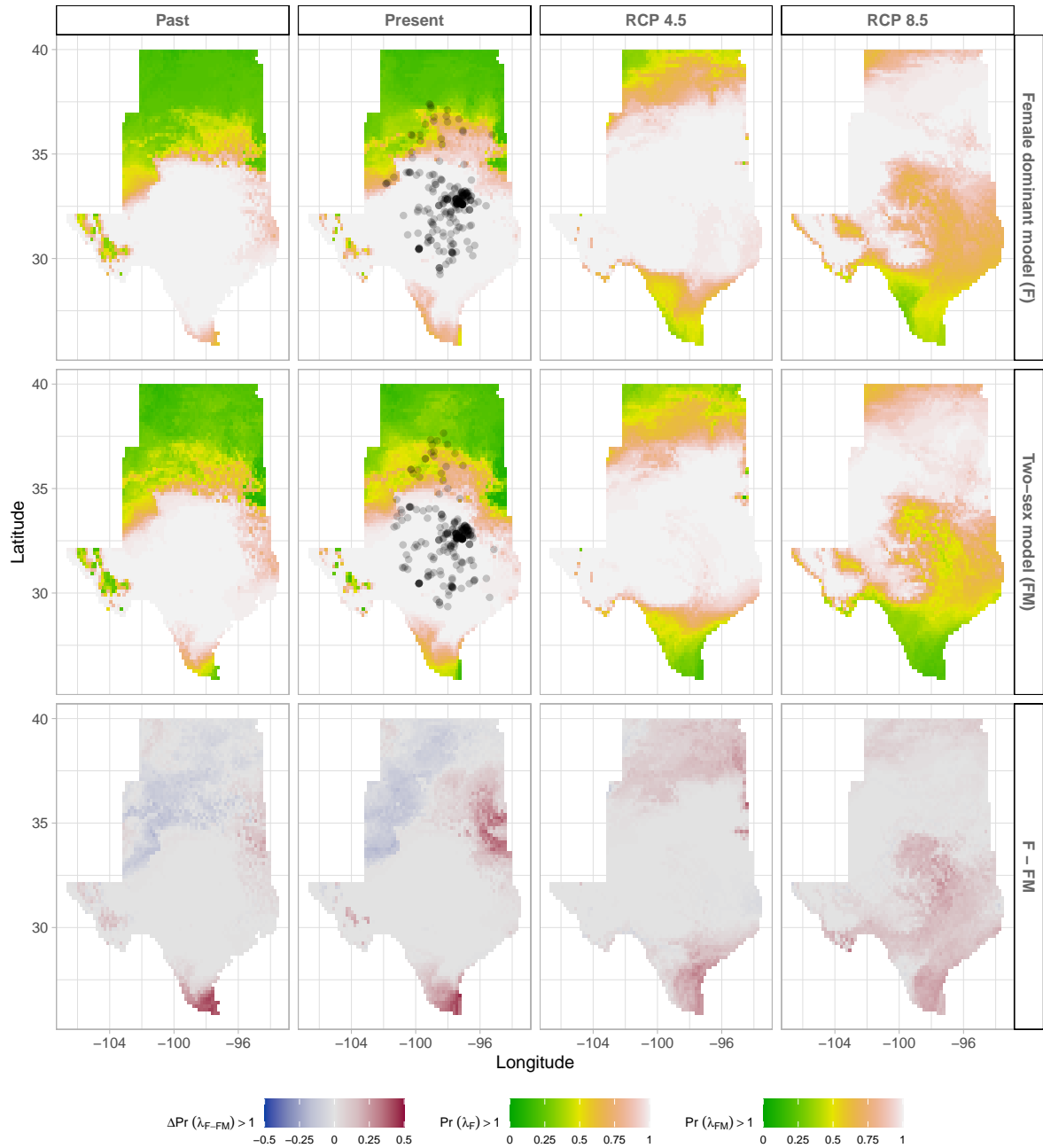


**Figure S-17:** Climate change favors range shift toward the North edge of the current range. (A) Past, (B) Current, (C and D) Future predicted range shift based on the predicted probabilities of self- sustaining populations,  $\Pr(\lambda > 1)$ , using the two-sex model that incorporates sex- specific demographic responses to climate with sex ratio dependent seed fertilization. (E) Past, (F) Current, (G and H) Future predicted range shift based on the predicted probabilities of self- sustaining populations,  $\Pr(\lambda > 1)$ , using the female dominant model. Future projections were based on the CESM1-BGC model. The black dots on panel B and F indicate all known presence points collected from GBIF from 1990 to 2019, which corresponds to the current condition in our prediction. The occurrences of GBIFs are distributed in with higher population fitness habitat  $\Pr(\lambda > 1)$  , confirming that our study approach can reasonably predict range shifts.

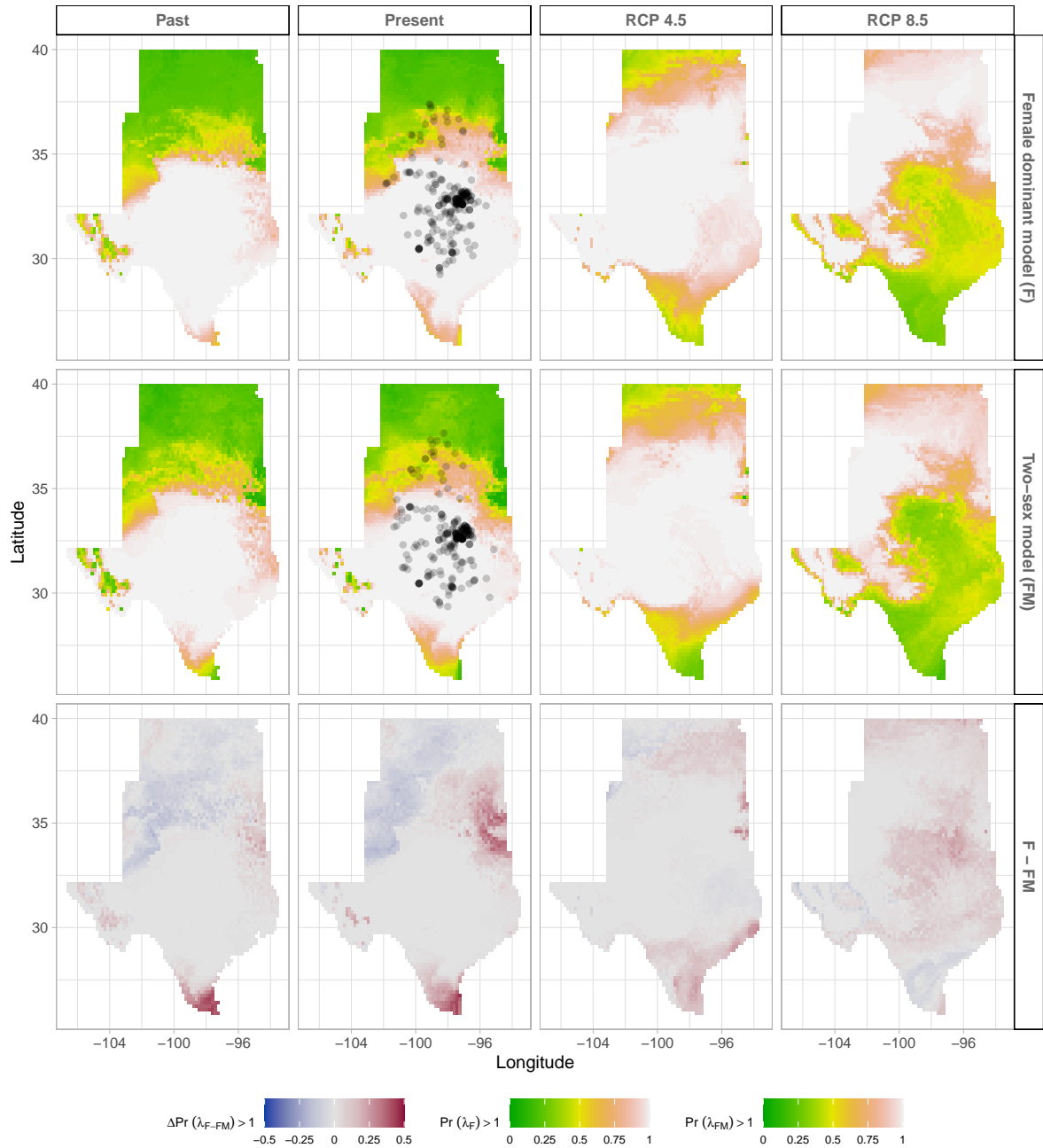


**Figure S-18:** Climate change favors range shift toward the North edge of the current range. (A) Past, (B) Current, (C and D) Future predicted range shift based on the predicted probabilities of self-sustaining populations,  $\text{Pr}(\lambda > 1)$ , using the two-sex model that incorporates sex-specific demographic responses to climate with sex ratio dependent seed fertilization. (E) Past, (F) Current, (G and H) Future predicted range shift based on the predicted probabilities of self-sustaining populations,  $\text{Pr}(\lambda > 1)$ , using the female dominant model. Future projections were based on the ACCESS model. The black dots on panel B and F indicate all known presence points collected from GBIF from 1990 to 2019, which corresponds to the current condition in our prediction. The occurrences of GBIFs are distributed in with higher population fitness habitat  $\text{Pr}(\lambda > 1)$ , confirming that our study approach can reasonably predict range shifts.

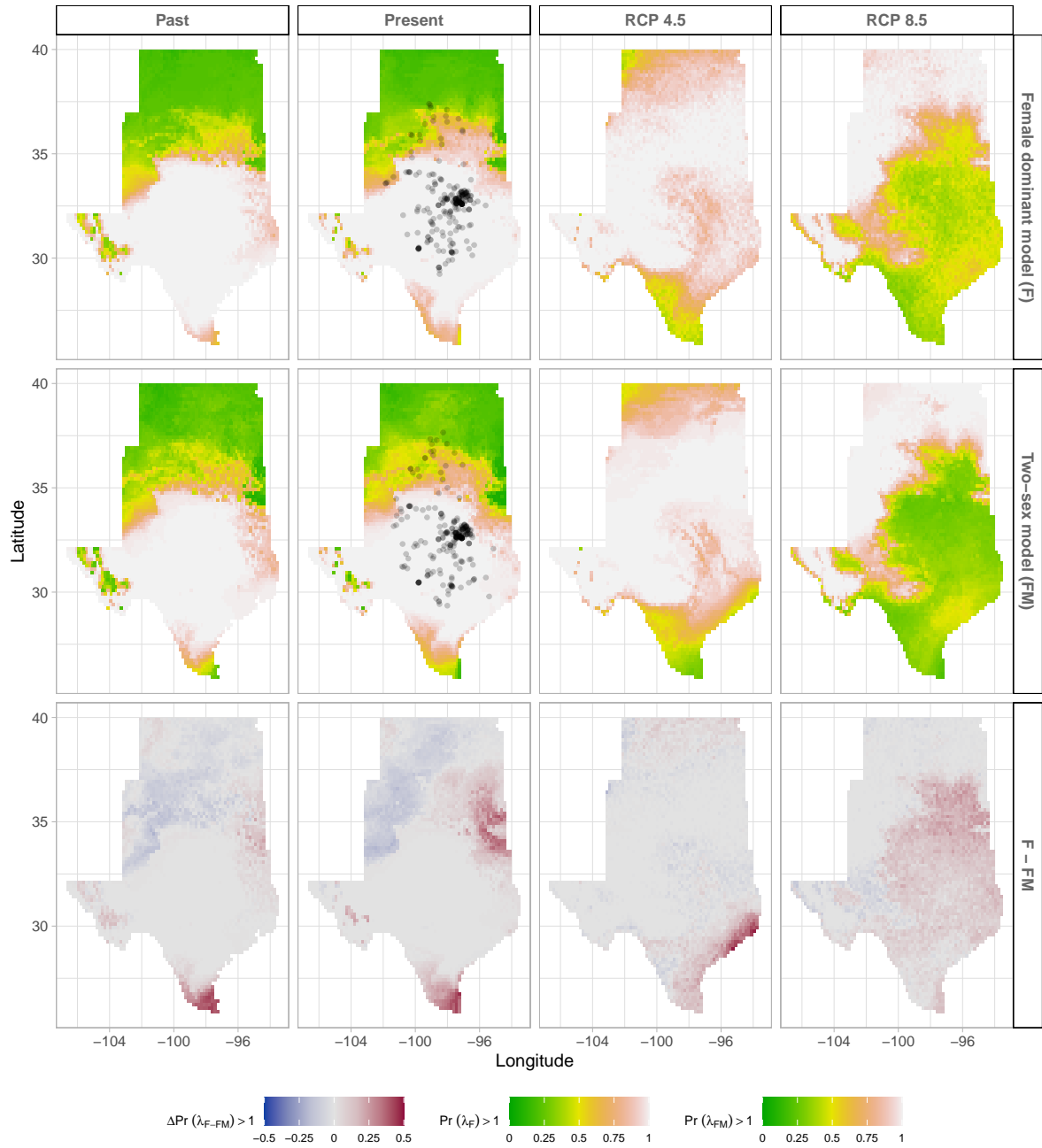


**Figure S-19:** Climate change favors range shift toward the North edge of the current range. (A) Past, (B) Current, (C and D) Future predicted range shift based on the predicted probabilities of self- sustaining populations,  $\text{Pr}(\lambda > 1)$ , using the two-sex model that incorporates sex- specific demographic responses to climate with sex ratio dependent seed fertilization. (E) Past, (F) Current, (G and H) Future predicted range shift based on the predicted probabilities of self- sustaining populations,  $\text{Pr}(\lambda > 1)$ , using the female dominant model. Future projections were based on the MIROC5 model. The black dots on panel B and F indicate all known presence points collected from GBIF from 1990 to 2019, which corresponds to the current condition in our prediction. The occurrences of GBIFs are distributed in with higher population fitness habitat  $\text{Pr}(\lambda > 1)$  , confirming that our study approach can reasonably predict range shifts.

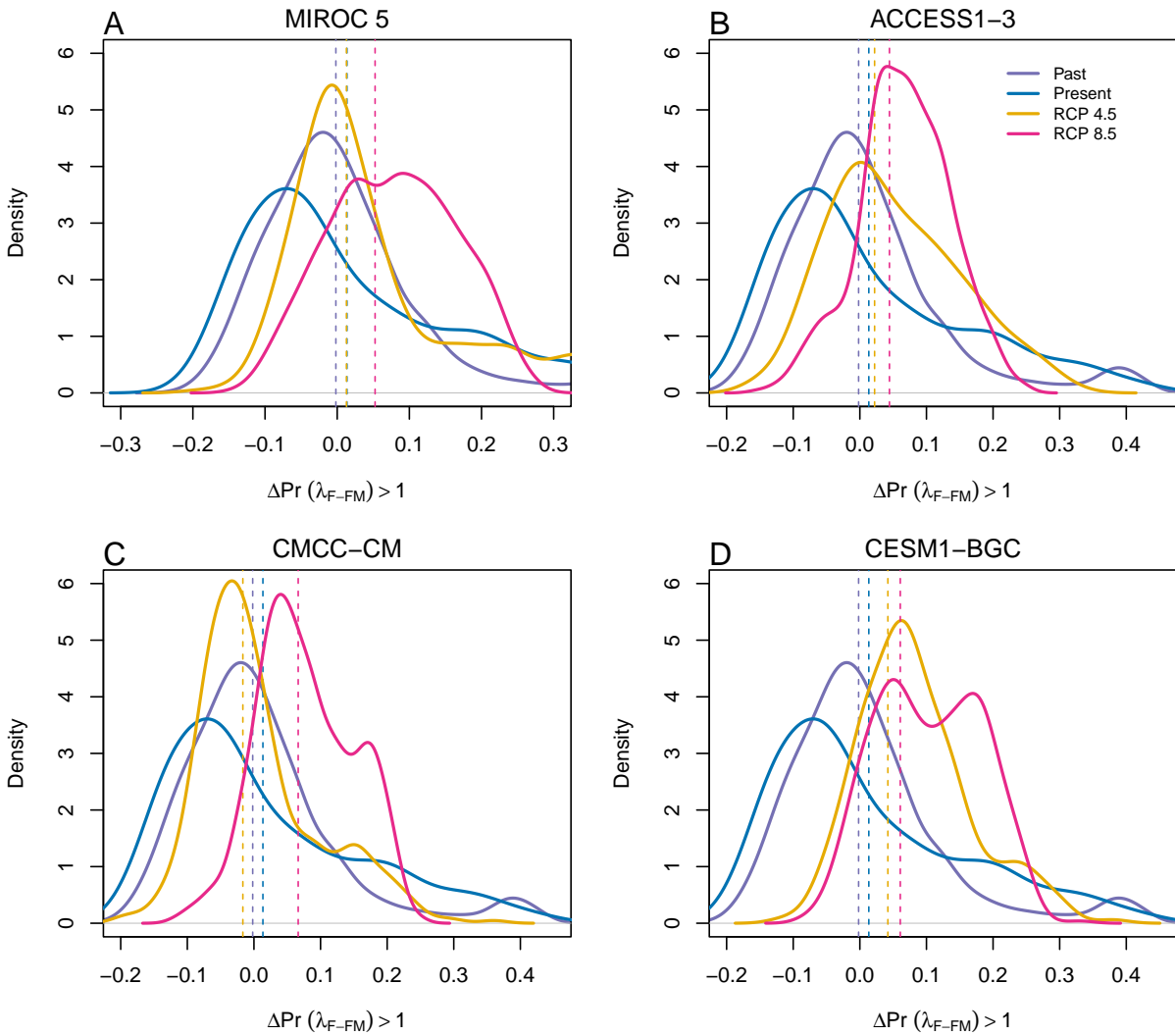


**Figure S-20:** Assessment of the statistical difference between the two-sex models and the female dominant model across and beyond species range for 4 GCMs. The means for each model are shown as vertical dashed lines.

651 **S.2 Supporting Methods**

652 **S.2.1 Sex-specific demographic responses to climatic variation across  
653 common garden sites**

Vital rate models were fit with the same linear predictors for the expected value ( $\mu$ )(Eq.S.1):

$$\begin{aligned} \mu = & \beta_0 + \beta_1 size + \beta_2 sex + \beta_3 pptgrow + \beta_4 pptdorm + \beta_5 tempgrow + \beta_6 tempdorm \\ & + \beta_7 pptgrow * sex + \beta_8 pptdorm * sex + \beta_9 tempgrow * sex + \beta_{10} tempdorm * sex \\ & + \beta_{11} size * sex + \beta_{12} pptgrow * tempgrow + \beta_{13} pptdorm * tempdorm \\ & + \beta_{14} pptgrow * tempgrow * sex + \beta_{15} pptdorm * tempdorm * sex + \beta_{16} pptgrow^2 \\ & + \beta_{17} pptdorm^2 + \beta_{18} tempgrow^2 + \beta_{19} tempdorm^2 + \beta_{20} pptgrow^2 * sex \\ & + \beta_{21} pptdorm^2 * sex + \beta_{22} tempgrow^2 * sex + \beta_{23} tempdorm^2 * sex + \phi + \rho + \nu \end{aligned} \quad (S.1)$$

654 where  $\beta_0$  is the grand mean intercept,  $\beta_1$  is the size dependent slopes. *size* was on a natural  
655 logarithm scale.  $\beta_2 \dots \beta_{13}$  represent the climate dependent slopes.  $\beta_{14} \dots \beta_{23}$  represent the  
656 sex-climate interaction slopes. *pptgrow* is the precipitation of the growing season, *tempgrow*  
657 is the temperature of the growing season, *pptdorm* is the precipitation of the dormant season,  
658 *tempdorm* is the temperature of the dormant season.

659 **S.2.2 Sex ratio responses to climatic variation across common garden sites**

To understand the impact of climatic variation across common garden sites on sex ratio, OSR and SR models using the same linear predictors for the expected value ( $\nu$ )(Eq.S.2):

$$\begin{aligned} \nu = & \omega_0 + \omega_1 pptgrow + \omega_2 pptdorm + \omega_3 tempgrow + \omega_4 tempdorm + \\ & \omega_5 pptgrow^2 + \omega_6 pptdorm^2 + \omega_7 tempgrow^2 + \omega_8 tempdorm^2 + \epsilon \end{aligned} \quad (S.2)$$

660 where *OSR* is the proportion of panicles that were female or proportion of female individuals  
661 in the experimental populations, *c* is the climate.  $\omega_0$  is the intercept,  $\omega_1, \dots, \omega_8$  are the climate  
662 dependent slopes.  $\epsilon$  is error term.

663 **S.2.3 Sex ratio experiment**

To estimate the probability of seed viability, the germination rate and the effect of sex-ratio variation on female reproductive success, we conducted a sex-ratio experiment at one site near the center of the range to estimate the effect of sex-ratio variation on female reproductive

success. The details of the experiment are provided in Compagnoni et al. (2017) and Miller and Compagnoni (2022b). Here we provide a summary of the experiment. We established 124 experimental populations in plots measuring 0.4 x 0.4m and separated by at least 15m from each other. We varied population density (1-48 plants/plot) and sex ratio (0%-100% female) across the experimental populations, and we replicated 34 combinations of density and sex ratio. We collected panicles from a subset of females in each plot and recorded the number of seeds in each panicle. We assessed reproductive success (seeds fertilized) using greenhouse-based germination and trazolium-based seed viability assays. Seed viability was modeled with a binomial distribution where the probability of viability ( $v$ ) was given by:

$$v = v_0 * (1 - OSR^\alpha) \quad (\text{S.3})$$

664 where  $OSR$  is the proportion of panicles that were female in the experimental populations.  
665  $\alpha$  is the parameter that control for how viability declines with increasing female bias. Further,  
666 germination rate was modeled using a binomial distribution to model the germination  
667 data from greenhouse trials. Given that germination was conditional on seed viability, the  
668 probability of success was given by the product  $v * g$ , where  $v$  is a function of  $OSR$  (Eq. S.3)  
669 and  $g$  is assumed to be constant.